# Presence of rapidly degrading permafrost plateaus in southcentral Alaska

Benjamin M. Jones[1], Carson A. Baughman[1], Vladimir E. Romanovsky[2,3], Andrew D. Parsekian[4], Esther L. Babcock[1], Eva Stephani[1], Miriam C. Jones[5], Guido Grosse[6], and Edward E. Berg[7]

[1] Alaska Science Center, U.S. Geological Survey, Anchorage, AK 99508, USA
[2] Geophysical Institute, University of Alaska Fairbanks, Fairbanks, AK 99775, USA
[3] Earth Cryosphere Institute, 86 Malygina Street, Tyumen 625000, Russia
[4] Department of Geology and Geophysics, University of Wyoming, Laramie, WY 82070, USA
[5] Eastern Geology and Paleoclimate Science Center, U.S. Geological Survey, Reston, VA 20192, USA
[6] Alfred Wegener Institute, Helmholtz Centre for Polar and Marine Research, Potsdam, 14473, Germany
[7] Kenai National Wildlife Refuge, U.S. Fish and Wildlife Service, Soldotna, AK 99669, USA (retired)

*Correspondence to*: Benjamin M. Jones (bjones@usgs.gov)

**Abstract.** Permafrost presence is determined by a complex interaction of climatic, topographic, and ecological conditions operating over long time scales. In particular, vegetation and organic layer characteristics may act to protect permafrost in regions with a mean annual air temperature (MAAT) above 0 °C. In this study, we document the presence of residual permafrost plateaus on the western Kenai Peninsula lowlands of southcentral Alaska, a region with a MAAT of 1.5±1 °C (1981–2010). Continuous ground temperature measurements between 16 September 2012 and 15 September 2015, using calibrated thermistor strings, documented the presence of warm permafrost (-0.04 °C to -0.08 °C). Field measurements (probing) on several plateau features during the fall of 2015 showed that the depth to the permafrost table averaged 1.48 m but at some locations was as shallow as 0.53 m. Late winter surveys (augering, coring, and GPR) in 2016 showed that the average seasonally frozen ground thickness was 0.45 m, overlying a talik above the permafrost table. Measured permafrost thickness ranged from 0.33 m to >6.90 m. Manual interpretation of historic aerial photography acquired in 1950 indicates that residual permafrost plateaus covered

920 ha as mapped across portions of four wetland complexes encompassing 4,810 ha. However, between 1950 and ca. 2010, permafrost plateau extent decreased by 60.0 %, with lateral feature degradation accounting for 85.0 % of the reduction in area. Permafrost loss on the Kenai Peninsula is likely associated with a warming climate, wildfires that remove the protective forest and organic layer cover, groundwater flow at depth, and lateral heat transfer from wetland surface waters in the summer. Better understanding the resilience and vulnerability of ecosystem-protected permafrost is critical for mapping and predicting future permafrost extent and degradation across all permafrost regions that are currently warming. Further work should focus on reconstructing permafrost history in southcentral Alaska as well as additional contemporary observations of these ecosystem-protected permafrost sites lying south of the regions with relatively stable permafrost.

## 1 Introduction

Permafrost is a major component of the cryosphere in the northern hemisphere, covering ~24 % of the terrestrial landscape (Brown et al., 1998). Permafrost is defined as ground that remains at or below 0 °C for at least two consecutive years (Van Everdingen, 1998). Four zones describe the lateral extent of permafrost regions: continuous (90–100 %), discontinuous (50–90 %), sporadic discontinuous (10–50 %), and isolated discontinuous (<10 %). This zonation typically represents the north to south changes in spatial distribution for terrestrial permafrost in high latitudes. Mean annual ground temperatures (MAGT) in the continuous permafrost zone can be as cold at -15 °C, fall within a narrow range around -2 °C in the discontinuous permafrost zone, and can be warmer than -1 °C in sporadic and isolated permafrost zones (Smith and Riseborough, 2002; Romanovsky et al., 2010; Smith et al., 2010). In the absence of extensive ground temperature data, researchers have estimated the southern limit of permafrost in northern high latitudes with continental-scale patterns of air temperature isotherms (Brown, 1960, 1970; Ferrians, 1965; Brown et al., 1998). However, in reality complex interactions between climatic, topographic, hydrologic, and ecologic conditions operating over long time scales regulate permafrost presence and stability (Shur and

Jorgenson, 2007).  Due to these interactions, permafrost may persist in regions with a mean annual

air temperature (MAAT) above 0 °C, and it may degrade in regions with a MAAT below -10 °C

(Jorgenson et al., 2010).  Thus, the extent and dynamics of permafrost and permafrost-related

landscape features remain poorly mapped and modelled at sufficiently fine resolution needed for

predicting the impact of climate change on specific local landscapes, which is necessary for many

decision makers.

Permafrost warming, degradation, and thaw subsidence can have significant implications

for ecosystems, infrastructure, and climate at local, regional, and global scales (Jorgenson et al.,

2001; Nelson et al., 2001; Schuur et al., 2008).  In general, permafrost in Alaska has warmed

between 0.3–6.0 °C since ground temperature measurements began between the 1950–1980s

(Lachenbruch and Marshall, 1986; Romanovsky and Osterkamp, 1995; Romanovsky et al., 2002;

Osterkamp, 2007; Romanovsky et al., 2010).  Warming and thawing of near-surface permafrost

may lead to widespread terrain instability in ice-rich permafrost in the Arctic (Jorgenson et al.,

2006; Lantz and Kokelj, 2008; Gooseff et al., 2009; Jones et al., 2015; Liljedahl et al., 2016) and

the sub-Arctic (Osterkamp et al., 2000; Jorgenson and Osterkamp, 2005; Lara et al., 2016).  Such

land surface changes can impact vegetation, hydrology, aquatic ecosystems, and soil-carbon

dynamics (Grosse et al., 2011; Jorgenson et al., 2013; Kokelj et al., 2015; O'Donnell et al., 2011;

Schuur et al., 2008; Vonk et al., 2015).  For example, in boreal peatlands, thaw of ice-rich

permafrost often converts forested permafrost plateaus into lake and wetland bog and fen

complexes (Camill, 1999; Jorgenson et al., 2001; Payette et al., 2004; Sannel and Kuhry 2008;

Sannel and Kuhry, 2011; Quinton et al., 2011; Jorgenson et al., 2012; Kanevskiy et al., 2014;

Swindles et al., 2015; Lara et al., 2016).  Furthermore, the transition from permafrost peatlands to

thawed or only seasonally frozen peatlands can have a positive or a negative feedback on regional

and global carbon cycles depending on permafrost conditions and differential effects of thaw on net primary productivity and heterotrophic respiration (Turetsky et al., 2007; Swindles et al., 2015), as well as on the degree of loss of the former deep permafrost carbon pool (O'Donnell et al., 2012).

In Alaska, a variety of permafrost conditions shape roughly 80 % of the landscape (Jorgenson et al., 2008). Shur and Jorgenson (2007) proposed five classes of permafrost that describe the interaction of climatological and ecological processes. Arranged from coldest to warmest, these permafrost classes are as follows: climate-driven; climate-driven but ecosystem-modified; climate-driven but ecosystem-protected; ecosystem-driven; and ecosystem-protected. Ecosystem-protected permafrost is the warmest and most vulnerable of the five classes of permafrost and characterizes the sporadic and isolated permafrost zones. It comprises residual permafrost that persists due to favourable ecosystem factors under a climate that is not conducive to its formation. Press disturbances, associated with warming air temperatures and increases in precipitation (especially snow), and pulse disturbances, such as fire or human activities, can trigger immediate ecosystem modification and permafrost thaw in these regions (Shur and Jorgenson, 2007).

Since permafrost acts as a sentinel, integrator, and regulator of climate change, improved understanding of its distribution and dynamics is essential, particularly along the southern permafrost boundary (Lunardini, 1996). Southcentral Alaska, a region with a MAAT ~2 °C, is typically mapped as being within the permafrost-free zone (Ferrians, 1965; Brown et al., 1998; Pastick et al., 2015). However, ecosystem-protected permafrost persists in southcentral Alaska in regions with present-day climatic conditions that are no longer conducive to its formation (Shur and Jorgenson, 2007). Isolated permafrost patches in southcentral Alaska exist on the western Kenai Peninsula Lowlands (Berg et al., 2009; Hopkins et al., 1955; Jorgenson et al., 2008) and in

the vicinity of Anchorage (Jorgenson et al., 2003; Riddle and Rooney, 2012; Kanevskiy et al., 2013). Enhanced insight into the resilience and vulnerability of ecosystem-protected permafrost is important due to its utility as a climate indicator and a forecaster of the environmental consequences expected to arise from permafrost thaw elsewhere in the boreal forest where MAAT is expected to warm beyond 0 °C in the coming decades (Beilman et al., 2001). Nevertheless, to date, detailed studies of these southcentral Alaska ecosystem-protected permafrost deposits have remained limited (Kanevskiy et al., 2013).

This study documents the presence of rapidly degrading permafrost plateaus on the western Kenai Peninsula lowlands of southcentral Alaska (Fig. 1), a region with a MAAT of 1.5±1 °C (Fig. 2). In mid-September 2012, we conducted field studies at several black spruce plateaus located within herbaceous wetland complexes. Continuous ground temperature measurements between 16 September 2012 and 15 September 2015 confirmed the presence and degradation of permafrost. Probing, drilling, coring, and ground-penetrating radar surveys conducted in the summer, fall, and winter seasons provided additional information on the geometry of the frozen ground below the forested plateaus. Historic aerial photography and high-resolution satellite imagery from 1950, 1984, 1996, and ca. 2010 were also used to map decadal-scale changes in the aerial extent of the residual permafrost plateaus in portions of four wetland complexes on the western Kenai Peninsula. This study aims to document and incorporate the loss of ecosystem-protected permafrost into the overall understanding of landscape dynamics on the western Kenai Peninsula lowlands. More importantly, insights into its stability will enhance mapping and predicting current and future permafrost extent along the southern fringe of the circumpolar permafrost region.

## 2 Study Area

The western Kenai Peninsula lowlands are located in southcentral Alaska, between 59.6–61.0 °N, and are generally less than 100 m above sea level (asl) (Fig. 1). The lowlands experience a semi-continental climate due to a rain shadow produced by the Kenai Mountains to the east and the presence of Cook Inlet to the west and north, and Kachemak Bay to the south (Jones et al., 2009). Regional MAAT for 1981–2010 was 1.5 °C, with a mean annual precipitation of 441 mm (http://www.ncdc.noaa.gov/crn/observations.htm) (Fig. 2). The lowlands represent a unique landscape where two major glacial ice fields converged during the Late Wisconsin, 25,000–21,000 kya (Reger et al., 2007). The modern topography, composed of moraines, outwash fans, kettle lakes, kames, and eskers, is indicative of this glacial history (Hopkins et al., 1955). During the Holocene, the Kenai Peninsula lowlands have succeeded to boreal forest, muskeg, and wetlands laced with rivers and creeks and dotted with lakes (Anderson et al., 2006; Reger et al., 2007). Pastick et al. (2015) recently mapped this region as being permafrost-free in the upper one meter of the ground surface.

The Kenai lowlands are situated in an ecotone between the coastal temperate rainforest and interior boreal forest. Species assemblages depend on topography and disturbance history, as well as their location relative to the rain shadow. Black spruce (*Picea mariana*), white spruce (*Picea glauca*), Sitka spruce (*Picea sitchensis*), Lutz spruce (*Picea x lutzii,* hybrid of white and Sitka spruce), paper birch (*Betula kenaica*), alder (*Alnus sp.*), black cottonwood (*Populus trichocarpa*), and aspen (*Populus tremuloides*) all occur within various forest stand types. Herbaceous and woody wetland complexes intermingle with these forests in low-lying areas and river corridors. Within wetland complexes, elevated forested plateaus, primarily black spruce but with some paper birch and cottonwood and an understory of dwarf shrubs, exist where the ground surface has been

elevated above the regional water table. We suspected these features were associated with a volumetric expansion of freezing peat, forming a permafrost plateau, an elevated permafrost feature associated with frost heave (Zoltai, 1972, Zoltai, 1993). Characterization of degrading permafrost plateaus is the focus of our studies on the Kenai Peninsula.

## 3 Methods

In September 2012, we conducted field studies at a number of black spruce plateaus located within herbaceous wetland complexes (Fig. 1, Fig. 3). These studies documented frozen ground below an unfrozen layer with thicknesses ranging from 0.49m to >1.00 m. The plateau features tended to have sharply defined scalloped edges, marginal thermokarst moats, and collapse-scar depressions on their summits (Fig. 3). These traits were characteristic of the permafrost features described by Hopkins et al. (1955) on the Kenai Peninsula and similar to permafrost plateaus across colder boreal regions (Zoltai, 1972; Thie, 1974; Jorgenson et al., 2001; Camill, 2005; Sannel et al., 2015). To answer whether the frozen deposits encountered at the black spruce plateaus were indeed permafrost, we collected continuous ground temperature measurements for three years, measured late-summer thaw depths, mechanically drilled and cored for the base of the frozen ground, imaged the subsurface with ground-penetrating radar (GPR), and analysed a time series of high-resolution remotely sensed imagery. These research efforts are described in more detail below.

### 3.1 Field Instrumentation and Surveys

To confirm the presence or absence of permafrost, data loggers were installed on 12 September 2012 at one ground temperature monitoring site in the Browns Lake and at three sites in the Watson Lake area (Fig. 1). A 5 cm diameter Kovacs Enterprise ice auger was used to drill the boreholes

167   and cased the holes with a 4.5 cm outer-diameter polyvinyl chloride (PVC) tube from the base of

168   the borehole to within 10 cm of the surface.  Each site was instrumented with a four channel Hobo

169   data logger (Onset U12-008) buried below the ground surface (bgs).  The data loggers recorded

170   hourly ground temperature at four depths from 0.10–3.00 m bgs using Hobo TMC1-HD and

171   TMC2-HD thermistors (Table 1).  The manufacturer-specified accuracy of the thermistors is ±0.25

172   °C.  Prior to deployment, we placed the data logger thermistors in a 0°C ice bath for up to 45

173   minutes to estimate a calibration factor for post-processing of the data following download in the

174   field.  After calibration in a 0°C ice bath, the precision of temperature measurements near 0 °C is

175   limited only by the sensor-logger system sensitivity, which is 0.031 °C in this case. Therefore, the

176   temperatures in our case were measured with the precision better than +/- 0.02 °C and changes in

177   soil temperature exceeding 0.031 °C can be recorded properly using this measuring system. This

178   fact was established and demonstrated many times during our measurements in deeper boreholes

179   using similar measuring systems when the annually measured temperature in some boreholes at

180   deeper depths (50 m and deeper) will remain constant.  These calibration techniques and

181   measurement sensitivities are similar to improvements recorded for other measurement systems

182   (Sannel et al., 2015; Cable et al., 2016).  All data were post-processed prior to summarizing the

183   hourly ground temperature data into daily, monthly, and annual means.

184       Additional field surveys at each study site provided information on the geometry of the

185   frozen ground distribution and deposit types. A tile probe was used to measure the depth to frozen

186   sediments at each ground temperature monitoring location in mid-September 2015 (limited to 2.2

187   m bgs). At the two forested plateaus in the Watson Lake wetland complex, tile probing locations

188   were selected randomly and split between hummock and depression microtopography.  At the

189   Browns Lake site, this depth was recorded at three points every meter along a 100 m transect across

190  the plateau feature. In addition, a topographic profile of the primary Browns Lake plateau was

191  collected using a Leica survey-grade differential GPS (dGPS) system (±0.02 m vertical accuracy)

192  on 09 October 2015 to adjust the probing measurements relative to the local topography. An

193  additional dGPS profile was acquired on 19 February 2016 at an adjacent plateau to provide more

194  relative feature height information in the wetland complex. At both the Browns Lake and Watson

195  Lake locations, the frozen ground thickness was measured using the Kovacs Enterprise ice auger

196  system powered by an 18V portable drill. At Browns Lake (site PF-BL-6), a borehole was also

197  core-drilled to a depth of 5.38 m using a SIPRE permafrost corer (5 cm diameter) with an engine

198  auger head for analysis of the frozen ground deposit (Fig. 1). The frozen cores were described

199  according to the cryofacies method (French and Shur, 2010) using cryostructure classification

200  systems inspired from Murton and French (1994) and Kanevskiy et al. (2014). Gravimetric ice

201  contents of eleven samples were measured by oven drying at 60 °C for 168 hours. Volumetric ice

202  contents were measured from ten well-preserved samples.

203      Implementation of GPR allowed to image certain characteristics of the frozen ground along

204  the primary Browns Lake plateau feature. A shielded 100 MHz Mala antenna was used in July

205  2014 and Sensors & Software 100 MHz unshielded bi-static antennas in common-offset

206  configuration in February 2016. The data were processed using commercially available Reflex-

207  W processing software (Sandmeier, 2008). Basic processing steps included dewow, time-zero

208  correction, removing bad traces, and bandpass filtering (40–67.2–128–369 MHz for Mala; 25–50–

209  200–400 MHz for Sensors & Software). Additional processing steps included an average

210  background subtraction with a running window of 20–100 traces to reduce noise from surface

211  multiples, where applicable, and variable gain for viewing purposes. Care was taken during

212  processing to preserve any flat-lying reflectors. Finally, the radargrams were corrected using the

213    dGPS surface topography and converted two-way travel time to depth using an estimated average

214    subsurface velocity of 0.038 m ns$^{-1}$ calibrated to average direct probe depths.

**3.2 Remotely Sensed Imagery and Change Detection**

216    Historic aerial photography and contemporary high resolution satellite imagery acquired between

217    1950–ca. 2010 provided an estimated extent of forested plateaus centred on four wetland

218    complexes on the western Kenai Peninsula lowlands.  Four change detection study areas (Fig. 1)

219    were selected based on the presence of forested-plateau features surrounded by herbaceous

220    wetland vegetation that likely indicated permafrost presence in the boreal wetlands on the Kenai

221    Peninsula (Hopkins et al., 1955).  Arranged from north to south, these included portions of the

222    Mystery Creek, Watson Lake, Browns Lake, and Tustumena Lake wetland complexes (Fig. 1).

223    Mapping forested plateau features and their change over time is a common method for detection

224    of permafrost thaw in boreal wetlands.  The land cover change associated with conversion of a

225    forested permafrost plateau to a lake or herbaceous wetland (i.e. bog or fen) is readily detectable

226    in high-resolution remotely sensed imagery (Thie, 1974; Camill and Clark, 1998; Osterkamp et

227    al., 2000; Jorgenson et al., 2001; Jorgenson et al., 2008; Payette et al., 2004; Quinton et al., 2011;

228    Lara et al., 2016).

229    A 25 km$^2$ square study area was overlaid at each of the potential permafrost areas and

230    clipped the wetland extent as defined by the 2001 National Land Cover Dataset for Alaska

231    (http://www.mrlc.gov/nlcd2011.php) to define the mapping area.  Panchromatic, Digital

232    Orthophoto Quadrangle (DOQs) images were produced at a spatial resolution of 1.0 m for the

233    entire Kenai Peninsula between July–August 1996.  The DOQs provided the base upon which to

234    georegister the other remotely sensed image datasets that consisted of panchromatic aerial photos

235    collected in August 1950 (1:40,000 scale), color-infrared aerial photos acquired in 1984 (1:62,500

236 scale), and panchromatic high-resolution satellite images (<1 m spatial resolution) acquired in ca.

237 2010. The mean RMS error associated with image georegistration was 1.82 m and ranged from

238 1.32–2.61 m. All images were sampled to a ground resolution of 1 m. Following image

239 registration, forested plateaus were manually digitized in a Geographic Information System

240 (ArcGIS v. 10.1) at a mapping scale of 1:1,000 (Fig. 4). The high-spatial resolution, georegistered

241 remotely sensed datasets allowed for the assessment of residual permafrost plateau extent in four

242 time slices (1950, 1984, 1996, ca. 2010) and change rates across three decadal-scale time periods:

243 (1) 1950–1984 (34 years), (2) 1984–1996 (12 years), and (3) 1996–ca. 2010 (14 years).

**3.3 Climate and Weather Data**

245 Climate and weather data were compiled from two regional stations to provide context for

246 interpreting the ground thermal regime data and changes mapped in the remotely sensed data.

247 Hourly air temperature data were compiled from Kenai Municipal Airport (KMA) (WBAN:

248 26523) for 1948–1971 and 1973–Present and sub-hourly air temperature data from the Kenai 29

249 ENE station (WBAN:26563) located at the Alaska Department of Fish and Game Moose Research

250 Center (MRC) from September 2010–Present. Since the MRC station is more representative of

251 the field study sites, the temperature record for MRC were reconstructed back to 1948 using a

252 linear regression function found between KMA and MRC daily mean temperatures as summarized

253 from hourly and sub-hourly measurements. The regression equation was calculated by comparing

254 daily mean temperature for 1 January 2012 to 31 December 2015, and validated against daily mean

255 temperatures at the MRC for 1 September 2010 to 31 December 2011. Lastly, daily snow depth

256 totals were acquired from September 2012–September 2015 from MRC records

257 (http://wcc.sc.egov.usda.gov/nwcc/site?sitenum=966).

**4 Results**

**4.1 Ground thermal regime of southcentral Alaska permafrost**

Calibrated ground temperature records collected between 16 September 2012 and 15 September 2015 at one forested plateau near Browns Lake and two forested plateaus near Watson Lake confirmed the presence of near-surface permafrost on the western Kenai Peninsula lowlands (Fig. 5a–5c). Over this time period, the MAGT of permafrost at 1.0 m bgs ranged from -0.04 °C to -0.08°C (Table 1). At the Browns Lake PF1 and the Watson Lake PF2 sites, permafrost at 2.0 m bgs had a MAGT between -0.06 °C and -0.08 °C. At the Browns Lake PF1 site, permafrost at 3.0 m bgs had a MAGT between -0.07 °C and -0.08 °C (Table 1). No permafrost was detected at a black spruce forested, non-plateau site near Watson Lake between September 2012 and August 2014 (Fig. 5d).

During the three-year observation period, an increase in near-surface ground temperatures was recorded at all three permafrost sites in response to increases in air temperature (Table 1, Fig. 5). The ground temperature at 0.5 m depth was substantially below 0 °C at all three sites during the 2012–2013 winter with minimum temperatures between -1.33 °C (Browns Lake) and -2.50 °C (Watson Lake PF2). In the 2013–2014 winter, the ground at 0.5 m depth was barely frozen at the Browns Lake and Watson Lake PF1 sites (Fig. 5a and 5b), with minimum winter temperatures at -0.32 °C and -0.20 °C, respectively. The increase in summer ground temperatures at 0.5 m depth was also substantial. By the end of the 2012 warm period, this temperature was above 0 °C only at the Browns Lake site (the maximum was at 0.40 °C). At the Watson Lake PF1 and PF2 sites the temperature at 0.5 m depth was just below 0 °C and never exceeded the thawing threshold, indicating that the maximum summer thaw (the active layer thickness) was just below 0.5 m during 2012. However, during the summer of 2013 and 2014, the active layer thickness was more than

281  0.5 m at both of these sites and the maximum temperatures in 2014 exceeded 1 °C at the Watson

282  Lake sites (Fig. 5b and 5c).  At the Browns Lake site the temperature at 0.5 m depth reached almost

283  2 °C before the thermistor malfunction.  The ground temperature warming at 0.5 m depth continued

284  in 2015 (Fig. 5b and 5c).

285      The increase in the shallow ground temperatures triggered warming in the near-surface

286  permafrost at all three permafrost sites (Fig. 6).  This warming was strong enough to initiate top-

287  down permafrost thaw at the Watson Lake PF1 site in the fall of 2014 (Fig. 6b).  Sensor failure

288  during the winter of 2014–2015 prevented further observations of ground temperature at this site

289  following thaw that winter.  At the Watson Lake PF2 site bottom-up permafrost thaw was detected

290  at a depth of 2 m during the fall of 2015 and likely associated with groundwater flow or degradation

291  of the permafrost in the thermokarst moat that borders the plateau.  At the Browns Lake site

292  permafrost persisted at the depths between 1.0–3.0 m bgs over the three-year observation period

293  (Fig. 6a).  However, MAGT warmed by 0.02 °C to 0.01 °C at all three depths during the

294  observation period.  The temperature at 1.0 m bgs is only -0.04 °C now.

295  **4.2 Depth to permafrost table and permafrost thickness**

296  The thaw depth at the data logger observation sites, as measured with the tile probe on 16

297  September 2015, was 0.64 m for the Watson Lake PF1 site (n=3), 0.53 m for the Watson Lake PF2

298  site (n=6), and 0.57 m for the Browns Lake PF1 site (n=6).  More systematic probing at all three

299  sites on 16 September 2015 showed that the average depth to the permafrost table where detectable

300  (max probe length=2.20 m) was 1.48 m (n=222).  However, probing did not encounter frozen

301  ground in the upper 2.20 m of the ground surface at an additional 140 measurement points, mostly

302  associated with collapse-scar features and thermokarst moats.  In general, depth to the permafrost

303  table depended on the local topographic conditions at each site.  Hummocks (n=164) tended to

304 have a shallower depth to the permafrost table where measureable (average of 1.12 m), while depth

305 to the permafrost table measurements in depressions (n=58) was larger (average of 1.53 m).

306       The measurements of the depth to permafrost table were complemented with mechanical

307 augering, coring, and GPR surveys in July 2014, September 2015, and February 2016 to constrain

308 permafrost thickness at the field observation sites. The most detailed measurements were collected

309 at the Browns Lake PF1 plateau feature (Fig. 7a). At this site, a topographic survey of the plateau

310 feature was conducted to plot depth to permafrost table along with seasonally frozen depth and

311 constraints on permafrost thickness in relation to the relative ground surface elevation along a 100

312 m transect (Fig. 7b). The relative mean elevation of the plateau above the surrounding wetland

313 area and the collapse-scar bog in the center was 0.49 m, with a maximum along the transect of

314 0.95 m, and a maximum across the feature of 1.30 m. A topographic survey on an adjacent plateau

315 feature produced a mean relative height of 0.59 m and a maximum of 1.81 m. We measured

316 permafrost thickness at five locations and minimum-limiting permafrost thicknesses at another

317 five locations along the Browns Lake primary plateau feature, with one limiting thickness

318 measurement at an adjacent plateau feature using the Kovacs auger. The base of the permafrost at

319 the two marginal plateau measurement sites at the primary plateau feature indicated a permafrost

320 thickness of 0.45 m and 0.33 m (Fig. 7b). At the three interior plateau measurements points,

321 permafrost was 5.57–5.65 m thick. At one of these locations (0.98 m relative height), a core was

322 acquired. It consisted of frozen peat from 0.48–5.69 m bgs, overlying 0.25 m of unfrozen peat,

323 with unfrozen mineral sediment at the base. At the other five locations where the bottom of

324 permafrost was not reached, drilling operations documented permafrost at least down to between

325 3.5–4.0 m bgs (Fig. 7b), and contained frozen peat as well.

326     The permafrost core at the PF-BL-6 site was described as poorly decomposed peat with

327     well-developed organic-matrix cryostructures, except between depths of 3.32–3.65 m where a

328     layer of silt and peat with mainly microlenticular cryostructure was observed (Fig. 8 and 9). The

329     gravimetric and volumetric ice contents of the peat varied between 883–1873 % and 80–96 %,

330     respectively, while they were 379–447 % and 81 %, respectively, in the previously mentioned silt

331     and peat layer. The upper two meters of peat were characterized mainly by an organic-matrix

332     porphyritic cryostructure transitioning to an organic-matrix microlenticular cryostructure with

333     some layered ice lenses. Below two meters, the peat was characterized mainly by an organic-

334     matrix microlenticular cryostructure with some belt-like and suspended cryostructures.

335     GPR surveys conducted in July 2014 and February 2016 provided more continuous

336     information on the geometry associated with the permafrost table in the residual plateaus on the

337     primary Browns Lake plateau feature (Fig. 10). The topography-corrected radargrams show a

338     prominent reflector between 1–3 m depth that coincides with the permafrost table in both the

339     summer (Fig. 10a) and winter (Fig. 10b) survey. The center portion of both images is characterized

340     by moderately continuous and chaotic reflectors (Neal, 2004), as expected for records in unfrozen

341     peat sequences (Parsekian et al., 2010) associated with the collapse-scar bog. The areas underlain

342     by permafrost (i.e. 0–30 m, 60–90 m) show subdued reflection events deeper than the permafrost

343     table; however, we were unable to image the permafrost base. The interpretation of these

344     radargrams provides lateral subsurface information on the presence of a talik overlying the

345     permafrost table.

346     **4.3 Remote identification of permafrost plateaus**

347     In 1950, residual permafrost plateau extent accounted for 920 ha of the 4,810 ha (19.1 %) of

348     wetlands mapped within four change detection areas (Fig. 1, Table 2). Between 1950 and 1984,

349     permafrost plateau extent decreased to 750 ha, at an average rate of 5.1 ha yr$^{-1}$ (Table 3).  Between

350     1984–1996, permafrost extent dropped to 520 ha, at an average rate of 18.8 ha yr$^{-1}$, the greatest

351     rate documented in the study periods. Between 1996–2010, permafrost features continued to

352     degrade at a rate of 9.5 ha yr$^{-1}$ so that by 2010, only 370 ha of the permafrost features remained.

353     Thus, between 1950–ca. 2010, 60 % of the residual permafrost plateaus disappeared in the mapped

354     study areas (Fig. 11 and Table 2).

355        Assessment of change in the four wetland complexes showed differences in the extent and

356     change rate of residual permafrost plateaus overtime.  The Mystery Creek study area had the most

357     extensive permafrost plateau coverage (32.8 % of the wetland area analysed) in the 1950s relative

358     to the Watson Lake (9.8 %), Browns Lake (11.1 %), and Tustumena Lake (15.8 %) study areas

359     (Table 2).  By ca. 2010, permafrost plateau extent in each of the study areas diminished to a cover

360     of 14.8 %, 3.5 %, 3.8 %, and 5.2 %, respectively.  Thus, there was a loss of 54.8 % of the plateau

361     extent in the Mystery Creek study area, 64.7 % in the Watson Lake study area, 65.5 % in the

362     Browns Lake study area, and 66.9 % in the Tustumena Lake study area between 1950–ca. 2010.

363     These changes equate to loss rates of 0.9 % yr$^{-1}$ for Mystery Creek and 1.1 % yr$^{-1}$ for the Watson,

364     Browns, and Tustumena Lake study areas (Table 3).  Mean area loss for all four sites was 0.8 %

365     yr$^{-1}$ between 1950 and 1984.  During this time, loss rate was greatest for Watson Lake and Brown

366     Lake and least for Mystery Creek.  Mean loss rate for all four sites increased to 2.3 % yr$^{-1}$ between

367     1984 and 1996.  During this time, loss rates were greatest in the north and least in the south with

368     Mystery Creek and Tustumena Lake losing 3.0 % yr$^{-1}$ and 1.2 % yr$^{-1}$, respectively. Average loss

369     rates decreased to 1.8 % yr$^{-1}$ between 1996 and 2010, with the three most northern sites losing

370     approximately 1.2 % yr$^{-1}$, while the Tustumena Lake study area lost 3.2 % yr$^{-1}$.  In terms of plateau

371     area lost per year within the three time periods, Mystery Creek (13.8 ha yr$^{-1}$), Watson Lake (1.6 ha

372  yr$^{-1}$), and Browns Lake (1.3 ha yr$^{-1}$) experienced the greatest areal loss rate during the 1984–1996

373  time period.  At the Tustumena Lake study area, the greatest rate of plateau extent loss (4.6 ha yr$^{-1}$

374  $^{1}$) occurred between 1996–ca. 2010 (Table 3).

375      This study also assessed whether the permafrost degradation occurred along the perimeter

376  of the plateau (marginal), whether degradation was internal to the plateau, or if complete

377  degradation of a plateau occurred.  Between 1950–2010, 85.0 % of the degradation occurred as

378  lateral thaw along the plateau margins, while internal thaw and complete loss of features accounted

379  for 1.5 % and 13.4 %, respectively.  Lateral loss of permafrost was greatest in the Watson Lake

380  study area (90.9 %) and least (77.0 %) in the Browns Lake study area.  Both Mystery Creek and

381  Tustumena Lake shared a lateral loss of 86.0 %.  Mystery Creek saw the greatest percent of internal

382  collapse loss (3.3 %) compared to Tustumena (1.7 %) and Watson and Browns Lake (both <1.0

383  %).  The complete loss of permafrost features was greatest in Browns Lake (22.4 %) and least in

384  Watson Lake (8.3 %).  Mystery Creek and Tustumena Lake had 10.5 % and 12.3 %, respectively,

385  of their permafrost plateaus disappear in the form of complete feature loss.  During the period of

386  remotely sensed observations complete feature loss increased from 6.7 % (1950–1984) to 21.0 %

387  (1996–ca. 2010) of the detected change, while lateral feature loss decreased from 91.0 % (1950–

388  1984) to 78.1 % (1996–ca. 2010) of the detected change, likely highlighting the role of

389  fragmentation promoting complete feature degradation.

390  **4.4 Climate and Weather Data**

391  The MAAT of the western Kenai Peninsula lowlands between 1981–2010 was 2.22 °C for the

392  KMA station and estimated to be 1.79 °C for the MRC station.  There was significant correlation

393  between the KMA and MRC daily mean air temperatures for the 2012–2015 period ($r^2$=0.97).  The

394  regression equation performed well during validation tests ($r^2$=0.95) and was therefore used to

395   estimate daily temperature data for the MRC station back to July 1948.  Mean annual air

396   temperature has increased by 0.4 °C since 1950, with a step increase occurring in 1976 associated

397   with the Pacific Decadal Oscillation (PDO) (Hartmann and Wendler, 2005) (Fig. 2).  Between July

398   1948 and December 1976, MAAT was 0.83 °C and 0.29°C for KMA and MRC, respectively.

399   Following the PDO shift MAAT increased to 1.97 °C and 1.51 °C for KMA and the MRC,

400   respectively (Fig. 2).  Prior to the PDO shift, 18 (MRC) and 6 (KMA) out of 27 years had a MAAT

401   below freezing and after the PDO shift, only 10 (MRC) and 0 (KMA) out of 39 years had a MAAT

402   below freezing.  MAAT at the MRC station was 0.88 °C (2012), 2.58 °C (2013), and 3.24 °C

403   (2014) during our three-year ground temperature observation period of 16 September 2012 to 15

404   September 2015.  Therefore, the observations during 2014–2015 occurred during a period with

405   anomalously high MAAT relative to the previous climate normal period, with more warming in

406   the winter than the summer months (Table 1).  Additionally, between 1948–2015, warm season

407   (May-September) air temperatures increased by 0.02 °C yr$^{-1}$ for both the Kenai and MRC station,

408   while winter season (October-April) air temperature increased by 0.04 °C yr$^{-1}$ (Table 4).

409

410   **5 Discussion**

411   **5.1 Presence of ecosystem-protected permafrost in southcentral Alaska**

412   These permafrost data for the residual permafrost plateaus on the Kenai Peninsula are the first such

413   observations for isolated permafrost bodies in southcentral Alaska (Osterkamp, 2007).  Based on

414   the five classes of permafrost proposed by Shur and Jorgenson (2007), the permafrost present in

415   wetland complexes of the western Kenai Peninsula lowlands is ecosystem-protected.  The

416   permafrost on the Kenai Peninsula is extremely warm, with a MAGT that ranges from -0.04 to -

417   0.08 °C (Table 1; Fig. 6).  Permafrost ground temperatures at all monitoring sites were near the

418  phase-equilibrium temperature at depths from 1.0–3.0 m. Latent-heat effects associated with

419  unfrozen water content in permafrost and with seasonal phase changes in the active layer can buffer

420  the ground thermal regime from changes in air temperature at warm permafrost sites (Romanovsky

421  and Osterkamp, 2000) and in part can explain the persistence of ecosystem-protected permafrost

422  on the Kenai Peninsula (Shur and Jorgenson, 2007; Jorgenson et al., 2010). Even though all

423  thermistors were calibrated prior to installation, the ability to resolve such warm permafrost

424  temperatures and their change over time using temperature alone is somewhat limiting. Thus,

425  future measurements at the residual permafrost plateau sites in southcentral Alaska will be

426  accompanied by the addition of soil moisture probes as well as borehole, nuclear magnetic

427  resonance (NMR) which provides a direct measure of liquid water content (Parsekian et al., 2013).

428      Field surveys that included probing, augering, coring and GPR provided additional

429  information on the vertical and spatial distribution of the warm permafrost on the western Kenai

430  Peninsula lowlands. The average active layer thickness at the permafrost plateau ground

431  temperature observation sites was 0.58 m. These sites were chosen for initial instrumentation in

432  September 2012 based in part on the relatively shallow depth to the frost table. More

433  comprehensive probing in September 2015 revealed that the average depth to the permafrost table

434  was 1.48 m (n=222) as averaged across three plateaus. At the Brown Lake plateau, a talik

435  overlying the permafrost table was present in February 2016. Average permafrost thickness at this

436  feature was 5.61 m thick, whereas at an adjacent feature it was more than 6.90 m, the maximum

437  depth of the auger flights. GPR survey data confirmed the presence of a continuous surface talik

438  at the Browns Lake site (Fig. 10); however, we were unable to image the base of the permafrost

439  using solely GPR, as similarly described by Lewkowicz et al. (2011). Based on visual

440  interpretation of the permafrost peat core acquired at the PF-BL-6 site in February 2016, the

441    permafrost deposit consists mainly of ice-rich frozen peat with well-developed organic-matrix

442    porphyritic and microlenticular cryostructures and some layered ice lenses, belt-like, and

443    suspended cryostructures (Fig. 8 and Fig. 9). Laboratory analysis also revealed gravimetric and

444    volumetric ice contents up to 1873 % and 96 %, respectively (Fig. 8).

445    **5.2 Extent and change in residual permafrost plateaus since the 1950s**

446    While previous reports of permafrost on the Kenai Peninsula exist (Hopkins et al., 1955; Jorgenson

447    et al., 2008), they were restricted to the wetland complex (Mystery Creek) north of Sterling (Berg

448    et al., 2009). Information on its dynamics here and elsewhere was lacking. The analysis of

449    remotely sensed imagery and field surveys identified residual permafrost plateaus in three

450    additional wetland complexes where it had not been previously identified (Fig. 1 and Fig. 11) and

451    indicated that the state of permafrost within the Kenai lowlands is highly dynamic. In 1950,

452    forested-permafrost plateau extent accounted for 19.0 % of the land cover in the 4,810 ha of

453    wetland complexes analysed in the four change detection study areas. In each of the wetland areas

454    analysed, permafrost plateaus accounted for more than 10.0 % of the area in 1950. However,

455    inferred permafrost extent decreased by 60.0 % between 1950–ca. 2010, and its lateral coverage

456    dropped below 5.0 % in three of the four study areas (Table 2).

457        The residual permafrost plateaus documented in this study share similar attributes to

458    features elsewhere in boreal peatlands for which permafrost degradation has been inferred due to

459    the ease of remotely detecting the conversion from forested permafrost plateau to non-permafrost

460    herbaceous wetland or waterbody (Jorgenson et al., 2001, 2008, 2012). Thie (1974) inferred a

461    permafrost plateau loss rate of 0.47 % $yr^{-1}$ between 1800–1960 for a 130,000 ha area of southern

462    Manitoba. In Québec, Canada, a 13 ha peat bog lost 1.80 % $yr^{-1}$ between 1957–2003 (Payette et

463    al., 2004). In the Northwest Territories, Canada, Quinton et al. (2011) reported a loss rate of 0.62

464   % yr$^{-1}$ between 1947–2008 across a 100 ha study area. In Interior Alaska (Tanana Flats), Jorgenson

465   et al. (2001) reported a loss rate of 0.76 % yr$^{-1}$ for birch forested permafrost plateaus between

466   1949–1995 using a point sampling method within a 260,000 ha wetland area. Lara et al. (2016)

467   recently updated these numbers for the Tanana Flats by manually digitizing features with methods

468   similar to ours and demonstrated that birch forest plateaus decreased at a much slower rate of 0.12

469   % yr$^{-1}$, and that black spruce forested permafrost plateau features appeared to be stable. Thus, the

470   loss rate of 1.0 % yr$^{-1}$ that we report for the 4,810 ha mapped on the western Kenai Peninsula

471   Lowlands between 1950–ca. 2010 are the second fastest change rates reported thus far in boreal

472   peatlands.

473   **5.3 Drivers of permafrost loss**

474   Permafrost on the Kenai Peninsula is likely degrading as a result of warming air temperatures (+0.4

475   °C decade$^{-1}$ since 1950), especially where warming during the winter season likely exacerbates

476   these effects (Table 4). During the three-year observation period as well as since the 1950s,

477   warming in the winter has been more pronounced than in the summer (Table 1 and Fig. 2) and

478   2014–2015 had a MAAT roughly double the 1981–2010 climate normal period. Storm systems

479   regularly bring warm air masses (>4 °C) to the region during the winter. Air temperature warming

480   during the winter months has decreased the number of freezing degree-days which means that the

481   ground freezes to a much lesser degree in the winter (Fig. 2 and Table 1). Therefore, ground

482   temperatures decreased less over the winter period (Fig. 5 and Table 1), potentially leading to talik

483   development. Previous research on permafrost plateaus in colder regions indicate that preferential

484   warming in the winter and increased snow accumulation leads to enhanced permafrost thaw in

485   boreal peatlands (Camill, 2005; Osterkamp, 2007). Since the Kenai Peninsula lowlands experience

486   a semi-continental climate due to the rain shadow produced by the Kenai Mountains, a lack of

487     winter snowfall may have contributed to permafrost persistence in this region by allowing

488     relatively cold winter air temperatures to propagate into the sub-surface. Thus, talik formation and

489     permafrost degradation at the study sites in southcentral Alaska are likely being driven for the most

490     part by winter air temperature warming (Fig. 2).

491            The increase in permafrost loss rate in southcentral Alaska following the 1980s is likely

492     due to the combined effects of forest fires and a shift in the PDO after 1976. The respective pulse

493     and press disturbances may have promoted large areas of permafrost already close to thawing, to

494     quickly thaw, leaving only colder permafrost and permafrost with intact peat and forest cover. Fire

495     can be an important driver of permafrost thaw (Yoshikawa et al., 2002) and thermokarst

496     development (Jones et al., 2015). The Kenai Fire of 1947 burned the majority of the Mystery

497     Creek study area, all of the Watson Lake study area, and the majority of the Browns Lake study

498     area. Evidence of this fire was seen at numerous sites in the Watson Lake and Browns Lake study

499     areas. Watson Lake and Browns Lake subsequently had the two greatest loss rates between 1950–

500     1984 which may be related to the 1947 fire. However, the presence of black spruce burn poles

501     were not found on all permafrost plateaus visited indicating that the burning was likely relatively

502     patchy in the wetlands. At Browns Lake, permafrost islands that did not burn in 1947 exhibited

503     less degradation, had thicker permafrost, denser tree cover, and larger trees than the islands that

504     burned. Large portions of the Tustumena Lake study area burned in the 1996 Crooked Creek Fire

505     and 2005 Fox Creek Fire. These fires likely damaged, and partially removed the protective

506     ecosystem cover (black spruce forest and peat), and degraded several permafrost plateau features.

507     This resulted in the Tustumena study area having the highest change rate for the latter time period

508     and 77.0 % of the plateau loss that occurred between 1996–ca. 2010 did so in areas that burned in

509     the 1996 and 2005 fires.

510     Bottom-up permafrost degradation was documented over the short period of direct

511     measurements between 2012–2015. The bottom-up permafrost thaw observed at the Watson Lake

512     PF2 site indicates that the flow of groundwater below the permafrost plateaus could be responsible

513     for degradation (Walters et al., 1998). In addition, analysis of the remotely sensed imagery for the

514     four select wetland complexes primarily documented lateral permafrost degradation since the

515     1950s, as inferred by the conversion of forested plateau margins to herbaceous wetland vegetation.

516     This type of feature loss accounted for 85.0% of the change between 1950–ca. 2010. This pattern

517     of loss was further observed in the field through the presence of thermokarst moats and drowning

518     black spruce trees along the margins of the permafrost plateaus (Fig. 3). This is similar to the

519     dominant processes documented in more northerly boreal peatlands with permafrost plateaus

520     (Thie, 1974; Camill and Clark, 1998; Osterkamp et al., 2000; Jorgenson et al., 2001; Payette et al.,

521     2004; Quinton et al., 2011; Jorgenson et al., 2012; O'Donnell et al., 2012; Lara et al., 2015). These

522     findings highlight the importance of groundwater flow and also the impact of saturated herbaceous

523     wetlands that absorb heat during the summer that likely degrades permafrost along the peat plateau

524     margins (Walters et al., 1998). It is possible that lateral permafrost degradation caused by these

525     processes is overwhelming the protection provided by the ecosystem cover for permafrost stability

526     on the Kenai Peninsula lowlands. Future research is required to more fully understand the role of

527     groundwater movement on permafrost instability in the study region.

528     **5.4 Proposed history of permafrost on the Kenai Peninsula**

529     During the Last Glacial Maximum (LGM), northern hemisphere permafrost extended much further

530     south than present day (Lindgren et al., 2015). However, permafrost history in southcentral Alaska

531     is poorly constrained. Even though the western Kenai Peninsula lowlands were almost completely

532     glaciated during the LGM (Reger et al., 2007), the permafrost features identified in this study occur

533  in glaciolacustrine or glaciofluvial wetland complexes that were either not glaciated during the

534  LGM (Mystery Creek) or became deglaciated before 16,000 cal yrs BP (Reger et al., 2007).

535  Perhaps permafrost formed on the Kenai Peninsula during deglaciation or shortly thereafter during

536  the Younger Dryas 12,900–11,700 years ago (Jones et al., 2009).  However, this permafrost would

537  have likely thawed during the Holocene Thermal Maximum (Zoltai, 1972; Kaufman et al., 2004).

538  As the regional climate became cooler and wetter, between 8,000–5,000 years ago, *Sphagnum*

539  accumulation and preservation on the western Kenai Peninsula lowlands may have promoted more

540  widespread permafrost aggradation (Jones et al., 2009).  Following this period, the peatlands may

541  have progressively froze, heaving the permafrost plateaus above the water table, drying the peat-

542  rich soils, promoting growth of black spruce, and creating a buffer layer protecting the underlying

543  permafrost (ecosystem-protected) from the unfavourable climate for permafrost that currently

544  exists today (Zoltai, 1972, 1995; Payette et al., 2004; Camill, 2005; Shur and Jorgenson, 2007).

545  Growth of permafrost and heaving the peatland surface above the water table could explain low

546  peat accumulation rates calculated in many Kenai Peninsula peatlands between 3,300–2,000 years

547  ago (Jones and Yu, 2010; Jones et al., 2014).  This also coincides with widespread neoglaciation

548  on the Kenai Peninsula 3,000–1,500 years ago (Wiles and Calkin, 1994, Barclay et al., 2009).

549  Alternatively, the Little Ice Age (365–165 years ago), promoted shallow permafrost formation in

550  areas that were predominantly unfrozen throughout the Holocene (Romanovsky et al., 1992;

551  Jorgenson et al., 2001), and thus, could account for the presence of residual permafrost on the

552  Kenai Peninsula.  The widespread loss of permafrost plateaus in central Alaska may be a result of

553  degradation of Little Ice Age permafrost (Jorgenson et al., 2001).  The age, history, and future

554  trajectory of permafrost on the western Kenai Peninsula lowlands require further study.

**5.5 Landscape dynamics and permafrost thaw on the western Kenai Peninsula lowlands**

Previous and ongoing land cover change on the western Kenai Peninsula lowlands are primarily in response to the interaction of climate change and human development. Increases in summer air temperature and late-summer droughts, along with human disturbance, have been linked to the massive spruce bark beetle (*Dendroctonus rufipennis*) outbreak of the late 1990s (Berg et al., 2006; Sherriff et al., 2011), which led to subsequent timber salvage (Jones, 2008). Berg and Anderson (2006) caution that overall drier conditions on the western Kenai Peninsula, combined with standing dead spruce stands, may alter the future fire regime of this region. Wetland drying (Klein et al., 2005) and establishment of woody vegetation in wetlands (Berg et al., 2009) may be attributed to warmer air temperatures and decreases in precipitation. Furthermore, tectonic activity associated with the Great Alaska Earthquake of 1964 caused the western Kenai Peninsula to lower in elevation by 0.7–2.3 m (Plafker, 1969), while the northern portion of the peninsula subsequently uplifted 0.8–0.9m (Cohen and Freymueller, 1997), potentially altering groundwater flow paths (Gracz, 2011).

In this study, the loss of ecosystem-protected permafrost in the overall understanding of landscape dynamics on the western Kenai Peninsula lowlands was documented and incorporated. The degradation of permafrost can impact terrestrial and aquatic ecosystems, hydrology, infrastructure, and carbon cycling on the Kenai Peninsula (Schuur et al., 2008; Grosse et al., 2011; Jorgenson et al., 2013; Kokelj et al., 2015; Vonk et al., 2015). Permafrost degradation within the wetlands is responsible for a shift from black spruce forest plateaus to fen and bog wetland ecosystems at a mean rate of 9.2ha $yr^{-1}$ since the 1950s in the four change detection study areas. Permafrost plateaus redirect surface and near-surface drainage in boreal wetlands (Quinton et al., 2011), and the thaw subsidence of these features increases drainage network connectivity (Beilman and Robinson, 2003), and alters the local hydrological cycle (Hayashi et al., 2007). Thus, the loss

579    of permafrost and/or changes in seasonally frozen ground phenology could in part be aiding in

580    observations of terrestrial and aquatic changes that have occurred on the Kenai Peninsula during

581    the past several decades.  Further work is required to better understand the past influence of

582    permafrost on the Kenai Peninsula as well as the future loss of these warm permafrost deposits.

583    **6 Conclusions**

584    Based on the ground data and remotely sensed observations, it was found that peatland permafrost

585    is currently more extensive than previously reported in southcentral Alaska, a region with a MAAT

586    of 1.5 °C.  Warm permafrost (-0.04 °C to -0.08 °C) persists on the western Kenai Peninsula

587    lowlands in forested (black spruce), peat plateaus found in glaciolacustrine and glaciofluvial

588    wetland complexes.  At the field study sites, the depth to permafrost table on the peat plateaus

589    averaged 1.48 m in September 2015, but was as shallow as 0.53 m at some locations.  Permafrost

590    thickness ranged from 0.33 m to greater than 6.90 m.  Field surveys conducted in February 2016

591    documented the presence of a surface talik overlying the permafrost table.  In 1950, residual

592    permafrost plateaus covered 19.0 % of the 4,810 ha wetland area mapped in the study.  Within the

593    changed detection study areas, 60.0 % of the permafrost plateaus present in 1950 had degraded by

594    ca. 2010.  In most cases, permafrost degradation equated to the loss of forest and its replacement

595    by bog or fen vegetation, preferentially occurring along permafrost plateau margins.  Permafrost

596    loss on the Kenai Peninsula is likely associated with a warming climate, particularly during the

597    winter season, wildfires that remove the protective ecosystem cover, groundwater flow at depth,

598    and lateral heat transfer from wetland surface waters in the summer.  Future studies on the residual

599    permafrost plateaus on the Kenai Peninsula will provide further insight for mapping and predicting

600    permafrost extent across Boreal permafrost regions that are currently warming.

## 7 Data availability

All data available upon request to the corresponding author.

## 8 Author contribution

B.M. Jones devised the study design and prepared the manuscript with contributions from all co-authors. B.M. Jones, C.A. Baughman, V.E. Romanovsky, E.L. Babcock, A.D. Parsekian, M.C. Jones, and E.E. Berg contributed to field instrumentation and field studies. B.M. Jones, C.A. Baughman, and G. Grosse conducted and contributed to remote sensing analysis. C.A. Baughman compiled and interpolated regional weather and climate station data. E.Stephani conducted the cryofacies analysis and laboratory testing. All co-authors contributed substantially to this research.

## 9 Acknowledgements

Funding for this research was provided by the U.S. Geological Survey Land Change Science and Land Remote Sensing programs. Support also was provided by the Russian Science Foundation (project RNF 16-17-00102). We thank the Kenai National Wildlife Refuge for granting permission to access field sites. We thank Kelly Harrell, Kobuk, Kashi, Lydia Zeglin, Josefine Lenz, Emiline Ostlind, and Callie Zuck for help with fieldwork. We thank David Swanson, Eric Klein, Neal Pastick, Mikhail Kanevskiy, and Andreas Kääb for providing useful feedback and edits on an earlier version of this paper. Any use of trade, product, or firm names is for descriptive purposes only and does not imply endorsement by the U.S. Government.

## 10 References

Allard M., Seguin M. K., and Levesque R.: Palsas and mineral permafrost mounds in northern Quebec, In International Geomorphology, Part II, Gardiner V (ed). John Wiley and Sons Ltd: Chichester; 285–309, 1986.

Anderson, R. S., Hallett, D. J., Berg, E., Jass, R. B., Toney, J. L., Fontaine, C. S. de and DeVolder, A.: Holocene development of Boreal forests and fire regimes on the Kenai Lowlands of Alaska, The Holocene, 16(6), 791–803, doi:10.1191/0959683606hol966rp, 2006.

Barclay, D.J., Wiles, G.C. and Calkin, P.E.: Holocene glacier fluctuations in Alaska. Quaternary Science Reviews, 28, 2034-2048, 2009.

Beilman, D. W. and Robinson, S. D.: Peatland permafrost thaw and landform type along a climatic gradient, Proc 8th Int Conf Permafr. Zurich Switz. 21–25 July 2003, 61 – 65, 2003.

Beilman, D. W., Vitt, D. H. and Halsey, L. A.: Localized Permafrost Peatlands in Western Canada: Definition, Distributions, and Degradation, Arct. Antarct. Alp. Res., 33(1), 70–77, doi:10.2307/1552279, 2001.

Berg, E. E. and Anderson, R. S.: Fire history of white and Lutz spruce forests on the Kenai Peninsula, Alaska, over the last two millennia as determined from soil charcoal, For. Ecol. Manag., 227(3), 275–283, doi:10.1016/j.foreco.2006.02.042, 2006.

Berg, E. E., David Henry, J., Fastie, C. L., De Volder, A. D. and Matsuoka, S. M.: Spruce beetle outbreaks on the Kenai Peninsula, Alaska, and Kluane National Park and Reserve, Yukon Territory: Relationship to summer temperatures and regional differences in disturbance regimes, For. Ecol. Manag., 227(3), 219–232, doi:10.1016/j.foreco.2006.02.038, 2006.

Berg, E. E., Hillman, K. M., Dial, R. and DeRuwe, A.: Recent woody invasion of wetlands on the Kenai Peninsula Lowlands, south-central Alaska: a major regime shift after 18 000 years of wet Sphagnum–sedge peat recruitment, Can. J. For. Res., 39(11), 2033–2046, doi:10.1139/X09-121, 2009.

Brown, J., Ferrians, O. J., Heginbottom, J. A. and Melnikov, E. S.: Circum-Arctic Map of Permafrost and Ground Ice Conditions, 1998.

Brown, R. J. E.: The Distribution of Permafrost and Its Relation to Air Temperature in Canada and the U.S.S.R., ARCTIC, 13(3), 163–177, doi:10.14430/arctic3697, 1960.

Brown, R. J. E.: Permafrost in Canada: its influence on Northern development, University of Toronto Press., 1970.

Cable, W. L., Romanovsky, V. E., and Jorgenson, M. T.: Scaling-up Permafrost Thermal Measurements in Western Alaska using an Ecotype Approach, The Cryosphere Discussions, doi:10.5194/tc-2016-30, 2016.

Camill, P.: Patterns of boreal permafrost peatland vegetation across environmental gradients sensitive to climate warming, Can. J. Bot., 77(5), 721–733, doi:10.1139/b99-008, 1999.

Camill, P.: Permafrost Thaw Accelerates in Boreal Peatlands During Late-20th Century Climate Warming, Clim. Change, 68(1–2), 135–152, doi:10.1007/s10584-005-4785-y, 2005.

Camill, P. and Clark, J. S.: Climate Change Disequilibrium of Boreal Permafrost Peatlands Caused by Local Processes, Am. Nat., 151(3), 207–222, doi: 10.1086/286112, 1998.

Cohen, S.C. and Freymueller, J.T.: Deformation of the Kenai Peninsula, Alaska, Journal of Geophysical Research: Solid Earth, 102, 20479-20487. 1997.

Ferrians, O. J.: Permafrost Map of Alaska, U.S. Geological Survey Miscellaneous Geologic Investigations Map I-445, scale 1:2,500,000, 1965.

Gooseff, M. N., Balser, A., Bowden, W. B. and Jones, J. B.: Effects of Hillslope Thermokarst in Northern Alaska, Eos Trans. Am. Geophys. Union, 90(4), 29–30, doi:10.1029/2009EO040001, 2009.

Gracz, M. B.: Comment on "Wetland drying and succession across the Kenai Peninsula Lowlands, south-central Alaska" Appears in Can. J. For. Res. 35: 1931-1941 (2005)., Can. J. For. Res., 41(2), 425–428, doi:10.1139/X10-147, 2011.

Grosse, G., Harden, J., Turetsky, M., McGuire, A. D., Camill, P., Tarnocai, C., Frolking, S., Schuur, E. A. G., Jorgenson, T., Marchenko, S., Romanovsky, V., Wickland, K. P., French, N., Waldrop, M., Bourgeau-Chavez, L. and Striegl, R. G.: Vulnerability of high-latitude soil organic carbon in North America to disturbance, J. Geophys. Res. Biogeosciences, 116(G4), G00K06, doi:10.1029/2010JG001507, 2011.

Hartmann, B., and Wendler, G.: The significance of the 1976 Pacific climate shift in the climatology of Alaska, Journal of Climate, 18(22), 4824–4839, 2005.

Hayashi, M., Goeller, N., Quinton, W. L. and Wright, N.: A simple heat-conduction method for simulating the frost-table depth in hydrological models, Hydrol. Process., 21(19), 2610–2622, doi:10.1002/hyp.6792, 2007.

Hopkins, D. M., Karlstrom, T. N. V., others, others and others: Permafrost and Ground Water in Alaska, Geological Survey Professional Paper, U.S. Geological Survey, United States Government Printing Office., 1955.

Jafarov, E. E., Romanovsky, V. E., Genet, H., McGuire, A. D. and Marchenko, S. S.: The effects of fire on the thermal stability of permafrost in lowland and upland black spruce forests of interior Alaska in a changing climate, Environ. Res. Lett., 8(3), 035030, doi:10.1088/1748-9326/8/3/035030, 2013.

Jones, B. M.: Land-cover change on the southern Kenai Peninsula lowlands, Alaska using USGS land cover trends methodology, J. Geogr. Reg. Plan., 1(4), 068–071, 2008.

Jones, B. M., Grosse, G., Arp, C. D., Miller, E., Liu, L., Hayes, D. J. and Larsen, C. F.: Recent Arctic tundra fire initiates widespread thermokarst development, Sci. Rep., 5, doi:10.1038/srep15865, 2015.

Jones, M. C., Peteet, D. M., Kurdyla, D. and Guilderson, T.: Climate and vegetation history from a 14,000-year peatland record, Kenai Peninsula, Alaska, Quat. Res., 72(2), 207–217, doi:10.1016/j.yqres.2009.04.002, 2009.

Jones, M.C. and Yu, Z.: Rapid deglacial and early Holocene expansion of peatlands in Alaska, Proceedings of the National Academy of Sciences, 107, 7347-7352, 2010.

Jones, M.C., Wooller, M. and Peteet, D.M.: A deglacial and Holocene record of climate variability in south-central Alaska from stable oxygen isotopes and plant macrofossils in peat, Quaternary Science Reviews, 87, 1–11, 2014.

Jorgenson, M. T., Racine, C. H., Walters, J. C. and Osterkamp, T. E.: Permafrost Degradation and Ecological Changes Associated with a Warming Climate in Central Alaska, Clim. Change, 48(4), 551–579, doi:10.1023/A:1005667424292, 2001.

Jorgenson, M. T. and Osterkamp, T. E.: Response of boreal ecosystems to varying modes of permafrost degradation, Can. J. For. Res., 35(9), 2100–2111, doi:10.1139/x05-153, 2005.

Jorgenson, M.T., Roth, J.E., Schlentner, S.F., Pullman, E.R. and Macander, M.: An ecological land survey for Fort Richardson, Alaska (No. ERDC/CRREL-TR-03-19). Engineer Research And Development Center Hanover Cold Regions Research And Engineering Lab, 2003.

Jorgenson, M. T., Shur, Y. L. and Pullman, E. R.: Abrupt increase in permafrost degradation in Arctic Alaska, Geophys. Res. Lett., 33(2), L02503, doi:10.1029/2005GL024960, 2006.

Jorgenson, T., Shur, Y.L., Osterkamp, T.E.: Thermokarst in Alaska. In Proceedings of the Ninth International Conference on Permafrost, Vol. 1, June 29–July 3, 2008, Fairbanks, Alaska, Kane DL, Hinkel KM (eds). Institute of Northern Engineering, University of Alaska Fairbanks; 869–876, 2008.

Jorgenson, M. T., Yoshikawa, K., Kanevskiy, M. Z., Shur, Y., Romanovsky, V. E., Marchenko, S., Grosse, G., Brown, J. and Jones, B. M.: Permafrost characteristics of Alaska, in 9th International Conference on Permafrost, 2008.

Jorgenson, M. T., Romanovsky, V., Harden, J., Shur, Y., O'Donnell, J., Schuur, E. A. G., Kanevskiy, M. and Marchenko, S.: Resilience and vulnerability of permafrost to climate change, Can. J. For. Res., 40(7), 1219–1236, doi:10.1139/X10-060, 2010.

Jorgenson, M.T., Kanevskiy, M., Shur, Y., Osterkamp, T., Fortier, D., Cater, T., Miller, P.: Thermokarst lake and shore fen development in boreal Alaska. In Proceedings of the Tenth International Conference on Permafrost, Vol. 1 International contributions, June 25–29, 2012, Salekhard, Russia, Hinkel KM (ed.). The Northern Publisher: Salekhard, Russia; 179–184, 2012.

Jorgenson, M. T., Harden, J., Kanevskiy, M., O'Donnell, J., Wickland, K., Stephanie Ewing, Manies, K., Zhuang, Q., Shur, Y., Striegl, R. and Koch, J.: Reorganization of vegetation, hydrology and soil carbon after permafrost degradation across heterogeneous boreal landscapes, Environ. Res. Lett., 8(3), 035017, doi:10.1088/1748-9326/8/3/035017, 2013.

Kanevskiy, M., Jorgenson, T., Shur, Y., O'Donnell, J.A., Harden, J.W., Zhuang, Q., and Fortier, D.: Cryostratigraphy and Permafrost Evolution in the Lacustrine Lowlands of West-Central Alaska, Permafrost and Periglacial Processes, 25(1), 14-34, 2014.

Kanevskiy, M., Shur, Y., Krzewinski, T. and Dillon, M.: Structure and properties of ice-rich permafrost near Anchorage, Alaska, Cold Reg. Sci. Technol., 93, 1–11, doi:10.1016/j.coldregions.2013.05.001, 2013.

Kaufman, D.S., Ager, T.A., Anderson, N.J., Anderson, P.M., Andrews, J.T., Bartlein, P.J., Brubaker, L.B., Coats, L.L., Cwynar, L.C., Duvall, M.L. and Dyke, A.S.: Holocene thermal maximum in the western Arctic (0–180 W). Quaternary Science Reviews, 23, 529–560, 2004.

Klein, E., Berg, E. E. and Dial, R.: Wetland drying and succession across the Kenai Peninsula Lowlands, south-central Alaska, Can. J. For. Res., 35(8), 1931–1941, doi:10.1139/x05-129, 2005.

Kokelj, S. V., Tunnicliffe, J., Lacelle, D., Lantz, T. C., Chin, K. S. and Fraser, R.: Increased precipitation drives mega slump development and destabilization of ice-rich permafrost terrain, northwestern Canada, Glob. Planet. Change, 129, 56–68, doi:10.1016/j.gloplacha.2015.02.008, 2015.

Lachenbruch, A. H. and Marshall, B. V.: Changing Climate: Geothermal Evidence from Permafrost in the Alaskan Arctic, Science, 234(4777), 689–696, doi:10.1126/science.234.4777.689, 1986.

Lantz, T. C. and Kokelj, S. V.: Increasing rates of retrogressive thaw slump activity in the Mackenzie Delta region, N.W.T., Canada, Geophys. Res. Lett., 35(6), L06502, doi:10.1029/2007GL032433, 2008.

Lara, M. J., Genet, H., McGuire, A. D., Euskirchen, E. S., Zhang, Y., Brown, D. R. N., Jorgenson, M. T., Romanovsky, V., Breen, A. and Bolton, W. R.: Thermokarst rates intensify due to climate change and forest fragmentation in an Alaskan boreal forest lowland, Glob. Change Biol., doi:10.1111/gcb.13124, 2015.

Lewkowicz, A.G., Etzelmüller, B. and Smith, S.L.: Characteristics of discontinuous permafrost based on ground temperature measurements and electrical resistivity tomography, southern Yukon, Canada, Permafrost and Periglacial Processes, 22(4), pp.320-342, 2011.

Liljedahl, A.K., Boike, J., Daanen, R.P., Fedorov, A.N., Frost, G.V., Grosse, G., Hinzman, L.D., Iijma, Y., Jorgenson, J.C., Matveyeva, N., , Necsoiu, M., , Raynolds, M. K., Romanovsky, V. E., Schulla, J., Tape, K., Walker, D. A., and H. Yabuki: Pan-Arctic ice-wedge degradation in warming permafrost and its influence on tundra hydrology, Nature Geoscience, 2016.

Lindgren, A., Hugelius, G., Kuhry, P., Christensen, T. R. and Vandenberghe, J.: GIS-based Maps and Area Estimates of Northern Hemisphere Permafrost Extent during the Last Glacial Maximum, Permafr. Periglac. Process., n/a–n/a, doi:10.1002/ppp.1851, 2015.

Lunardini, V.J.: Climatic warming and the degradation of warm permafrost. Permafrost and Periglacial Processes, 7(4), 311-320, 1996.

Lynch, J. A., Clark, J. S., Bigelow, N. H., Edwards, M. E. and Finney, B. P.: Geographic and temporal variations in fire history in boreal ecosystems of Alaska, J. Geophys. Res. Atmospheres, 107(D1), 8152, doi:10.1029/2001JD000332, 2002.

769 Morse, P. D., Wolfe, S. A., Kokelj, S. V. and Gaanderse, A. J. R.: The Occurrence and Thermal
770     Disequilibrium State of Permafrost in Forest Ecotopes of the Great Slave Region, Northwest
771     Territories, Canada, Permafr. Periglac. Process., doi:10.1002/ppp.1858, 2015.

772 Murton, J.B, and French, H.M.: Cryostructures in permafrost, Tuktoyaktuk coastlands, western
773     Arctic Canada. Canadian Journal of Earth Sciences, 31, pp.737–747, 1994.

774 Neal, A.: Ground-penetrating radar and its use in sedimentology: principles, problems and
775     progress, Earth-science reviews, 66, 261-330, 2004.

776 Nelson, F. E., Anisimov, O. A. and Shiklomanov, N. I.: Subsidence risk from thawing permafrost,
777     Nature, 410(6831), 889–890, doi:10.1038/35073746, 2001.

778 O'Donnell, J.A., Harden, J.W., McGuire, A.D., Kanevskiy, M.Z., Jorgenson, M.T., Xu, X. The
779     effect of fire and permafrost interactions on soil carbon accumulation in an upland black
780     spruce ecosystem of interior Alaska: implications for post-thaw carbon loss. Global Change
781     Biology 17: 1461–1474. DOI: 10.1111/j.1365-2486. 2010.02358, 2011.

782 O'Donnell, J. A., Jorgenson, M. T., Harden, J. W., McGuire, A. D., Kanevskiy, M. Z. and
783     Wickland, K. P.: The Effects of Permafrost Thaw on Soil Hydrologic, Thermal, and Carbon
784     Dynamics in an Alaskan Peatland, Ecosystems, 15(2), 213–229, doi:10.1007/s10021-011-
785     9504-0, 2012.

786 Osterkamp, T. E.: Characteristics of the recent warming of permafrost in Alaska, J. Geophys. Res.
787     Earth Surf., 112(F2), F02S02, doi:10.1029/2006JF000578, 2007.

788 Osterkamp, T. E., Viereck, L., Shur, Y., Jorgenson, M. T., Racine, C., Doyle, A. and Boone, R.
789     D.: Observations of Thermokarst and Its Impact on Boreal Forests in Alaska, U.S.A., Arct.
790     Antarct. Alp. Res., 32(3), 303–315, doi:10.2307/1552529, 2000.

791 Parsekian, A. D., Slater, L., Comas, X., and Glaser, P. H.: Variations in free-phase gases in peat
792     landforms determined by ground-penetrating radar, Journal of Geophysical Research:
793     Biogeosciences, 115, no. G2, 2010.

794 Parsekian, A.D., Grosse, G., Walbrecker, J.O., Müller-Petke, M., Keating, K., Liu, L., Jones, B.M.
795     and Knight, R.: Detecting unfrozen sediments below thermokarst lakes with surface nuclear
796     magnetic resonance, Geophysical Research Letters, 40(3), 535-540, 2013.

797 Pastick, N. J., Jorgenson, M. T., Wylie, B. K., Nield, S. J., Johnson, K. D. and Finley, A. O.:
798     Distribution of near-surface permafrost in Alaska: Estimates of present and future conditions,
799     Remote Sens. Environ., 168, 301–315, doi:10.1016/j.rse.2015.07.019, 2015.

Payette, S., Delwaide, A., Caccianiga, M. and Beauchemin, M.: Accelerated thawing of subarctic peatland permafrost over the last 50 years, Geophys. Res. Lett., 31(18), L18208, doi:10.1029/2004GL020358, 2004.

Plafker, G.: Tectonics of the March 27, 1964 Alaska earthquake: U.S. Geological Survey Professional Paper. [online] Available from: http://pubs.usgs.gov/pp/0543i/, 1969.

Quinton, W. l., Hayashi, M. and Chasmer, L. e.: Permafrost-thaw-induced land-cover change in the Canadian subarctic: implications for water resources, Hydrol. Process., 25(1), 152–158, doi:10.1002/hyp.7894, 2011.

Reger, R. D., Sturmann, A. G., Berg, E. E. and Burns, P. A. C.: A guide to the late Quaternary history of northern and western Kenai Peninsula, Alaska: Alaska Division of Geological & Geophysical Surveys Guidebook 8, 2007.

Riddle, C.H., Rooney, J.W.: Encounters with relict permafrost in the Anchor- age, Alaska, area. Proceedings of the Tenth International Conference on Permafrost, Salekhard, Yamal-Nenets Autonomous District, Russia, June 25–29, 2012, 1, pp. 323–328, 2012.

Romanovsky, V. E., Garagula, L. S., and Seregina, N. V.: Freezing and thawing of soils under the influence of 300- and 90-year periods of temperature fluctuation. Pages 543–548 in Proceedings of the International Conference on the Role of Polar Regions in Global Change. Fairbanks (AK): Geophysical Institute, University of Alaska. 1992.

Romanovsky, V. E. and Osterkamp, T. E.: Effects of unfrozen water on heat and mass transport processes in the active layer and permafrost, Permafr. Periglac. Process., 11(3), 219–239, doi:10.1002/1099-1530(200007/09)11:3<219::AID-PPP352>3.0.CO;2-7, 2000.

Romanovsky, V. E. and Osterkamp, T. E. (1995), Interannual variations of the thermal regime of the active layer and near-surface permafrost in northern Alaska. Permafrost Periglac. Process., 6: 313–335. doi: 10.1002/ppp.3430060404

Romanovsky, V., Burgess, M., Smith, S., Yoshikawa, K. and Brown, J.: Permafrost temperature records: Indicators of climate change, Eos Trans. Am. Geophys. Union, 83(50), 589–594, doi:10.1029/2002EO000402, 2002.

Romanovsky, V. E., Smith, S. L. and Christiansen, H. H.: Permafrost thermal state in the polar Northern Hemisphere during the international polar year 2007–2009: a synthesis, Permafr. Periglac. Process., 21(2), 106–116, doi:10.1002/ppp.689, 2010.

830  Sandmeier, K. J.: REFLEXW – WindowsTM 9x/NT/2000/XP-program for the processing of
831      seismic, acoustic or electromagnetic reflection, refraction and transmission data, 2008.

832  Sannel, A.B.K., Kuhry, P. : Long-term stability of permafrost in subarctic peat plateaus, west-
833      central Canada. The Holocene 18, 589–601, 2008.

834  Sannel, A.B.K., Kuhry, P.: Warming induced destabilization of peat plateau/thermokarst lake
835      complexes. Journal of Geophysical Research 116, G03035, doi:10.1029/2010JG001635,
836      2011.

837  Sannel, A. B. K., Hugelius, G., Jansson, P. and Kuhry, P.: Permafrost Warming in a Subarctic
838      Peatland – Which Meteorological Controls are Most Important?, Permafr. Periglac. Process.,
839      n/a–n/a, doi:10.1002/ppp.1862, 2015.

840  Schuur, E. A. G., Bockheim, J., Canadell, J. G., Euskirchen, E., Field, C. B., Goryachkin, S. V.,
841      Hagemann, S., Kuhry, P., Lafleur, P. M., Lee, H., Mazhitova, G., Nelson, F. E., Rinke, A.,
842      Romanovsky, V. E., Shiklomanov, N., Tarnocai, C., Venevsky, S., Vogel, J. G. and Zimov,
843      S. A.: Vulnerability of Permafrost Carbon to Climate Change: Implications for the Global
844      Carbon Cycle, BioScience, 58(8), 701–714, doi:10.1641/B580807, 2008.

845  Sherriff, R. L., Berg, E. E. and Miller, A. E.: Climate variability and spruce beetle (Dendroctonus
846      rufipennis) outbreaks in south-central and southwest Alaska, Ecology, 92(7), 1459–1470,
847      doi:10.1890/10-1118.1, 2011.

848  Shur, Y. L. and Jorgenson, M. T.: Patterns of permafrost formation and degradation in relation to
849      climate and ecosystems, Permafr. Periglac. Process., 18(1), 7–19, doi:10.1002/ppp.582, 2007.

850  Smith, M. W. and Riseborough, D. W.: Climate and the limits of permafrost: a zonal analysis,
851      Permafr. Periglac. Process., 13(1), 1–15, doi:10.1002/ppp.410, 2002.

852  Swindles, G.T., Morris, P.J., Mullan, D., Watson, E.J., Turner, T.E., Roland, T.P., Amesbury, M.J.,
853      Kokfelt, U., Schoning, K., Pratte, S. and Gallego-Sala, A.: The long-term fate of permafrost
854      peatlands under rapid climate warming, Scientific Reports, 5, 17951, 10.1038/srep17951,
855      2015.

856  Thie, J.: Distribution and Thawing of Permafrost in the Southern Part of the Discontinuous
857      Permafrost Zone in Manitoba, ARCTIC, 27(3), 1974.

858  Turetsky, M. R., Wieder, R. K., Vitt, D. H., Evans, R. J. and Scott, K. D.: The disappearance of
859      relict permafrost in boreal North America: Effects on peatland carbon storage and fluxes,
860      Glob. Change Biol., 13(9), 1922–1934, doi:10.1111/j.1365-2486.2007.01381.x, 2007.

Van Everdingen, R. O.,: Multi-Language Glossary of Permafrost and Related Ground-Ice Terms in Chinese, English, French, German, Icelandic, Italian, Norwegian, Polish, Romanian, Russian, Spanish, and Swedish. International Permafrost Association, Terminology Working Group, 1998.

Vonk, J. E., Tank, S. E., Bowden, W. B., Laurion, I., Vincent, W. F., Alekseychik, P., Amyot, M., Billet, M. F., Canário, J., Cory, R. M., Deshpande, B. N., Helbig, M., Jammet, M., Karlsson, J., Larouche, J., MacMillan, G., Rautio, M., Walter Anthony, K. M. and Wickland, K. P.: Reviews and syntheses: Effects of permafrost thaw on Arctic aquatic ecosystems, Biogeosciences, 12(23), 7129–7167, doi:10.5194/bg-12-7129-2015, 2015.

Walters J.C., Racine C.H., and Jorgenson M.T.: Characteristics of permafrost in the Tanana Flats, interior Alaska, In: Proceedings of the Seventh International Conference on Permafrost Vol 57 (eds. Lewkowicz AG, Allard M), Université Laval, Québec. Collection Nordicana, 1109–1116, 1998.

Wiles, G. C. and Calkin, P. E.: Late Holocene, high-resolution glacial chronologies and climate, Kenai Mountains, Alaska, Geol. Soc. Am. Bull., 106(2), 281–303, doi:10.1130/0016-7606(1994)106<0281:LHHRGC>2.3.CO;2, 1994.

Yoshikawa, K., Bolton, W. R., Romanovsky, V. E., Fukuda, M. and Hinzman, L. D.: Impacts of wildfire on the permafrost in the boreal forests of Interior Alaska, J. Geophys. Res. Atmospheres, 107(D1), 8148, doi:10.1029/2001JD000438, 2002.

Zoltai, S. C.: Palsas and Peat Plateaus in Central Manitoba and Saskatchewan, Can. J. For. Res., 2(3), 291–302, doi:10.1139/x72-046, 1972.

Zoltai, S.C.: Cyclic development of permafrost in the peatlands of northwestern Alberta, Canada. Arctic and Alpine Research 25, 240–246, 1993.

Zoltai, S. C.: Permafrost Distribution in Peatlands of West-Central Canada During the Holocene Warm Period 6000 Years BP, Géographie Phys. Quat., 49(1), 45, doi:10.7202/033029ar, 1995.

**Tables**

Table 1. Mean annual ground temperature (MAGT) data for four observation sites on the Kenai Peninsula lowlands. Browns Lake PF1, Watson Lake PF1, and Watson Lake PF2 represent permafrost plateaus and the Watson Lake non-PF site a black spruce forested non-plateau site. Sensor depths that were perennially frozen in a given year are in bold. Mean annual air temperature (MAAT), thawing and freezing degree days (TDD and FDD), and average winter snow depth (MASD) are from the he MRC station (Kenai 29 ENE - AWS 702590).

**9/16/2012 - 9/15/2013**

| Browns Lake PF1 | | Watson Lake PF1 | | Watson Lake PF2 | | Watson Lake non-PF | | KENAI 29 ENE AWS 702590 Met Station Data | | | |
|---|---|---|---|---|---|---|---|---|---|---|---|
| Sensor depth (cm) | MAGT (°C) | Sensor depth (cm) | MAGT (°C) | Sensor depth (cm) | MAGT (°C) | Sensor depth (cm) | MAGT (°C) | MAAT (°C) | TDD Sums | FDD Sums | MASD (cm) |
| 50 | -0.02 | 10 | 0.34 | 10 | 0.05 | 25 | 0.94 | | | | |
| **100** | **-0.06** | 25 | -0.09 | 50 | -0.30 | 50 | 0.42 | 0.88 | 1865.9 | 1544.3 | 19.3 |
| **200** | **-0.08** | 50 | -0.20 | **100** | **-0.08** | 100 | 0.14 | | | | |
| **300** | **-0.08** | **100** | **-0.08** | **200** | **-0.06** | 130 | 0.16 | | | | |

**9/16/2013 - 9/15/2014**

| Browns Lake PF1 | | Watson Lake PF1 | | Watson Lake PF2 | | Watson Lake non-PF | | KENAI 29 ENE AWS 702590 Met Station Data | | | |
|---|---|---|---|---|---|---|---|---|---|---|---|
| Sensor depth (cm) | MAGT (°C) | Sensor depth (cm) | MAGT (°C) | Sensor depth (cm) | MAGT (°C) | Sensor depth (cm) | MAGT (°C) | MAAT (°C) | TDD Sums | FDD Sums | MASD (cm) |
| 50* | 0.17 | 10 | 0.93 | 10 | 0.86 | 25 | 0.57 | | | | |
| **100** | **-0.06** | 25 | 0.40 | 50 | -0.07 | 50 | 0.32 | 2.58 | 2066.6 | 1123.4 | 8.3 |
| **200** | **-0.06** | 50 | -0.02 | **100** | **-0.08** | 100 | 0.14 | | | | |
| **300** | **-0.08** | **100** | **-0.06** | **200** | **-0.08** | 130 | 0.14 | | | | |

*Thermistor failed on 24 August 2014

**9/16/2014 - 9/15/2015**

| Browns Lake PF1 | | Watson Lake PF1 | | Watson Lake PF2 | | Watson Lake non-PF | | KENAI 29 ENE AWS 702590 Met Station Data | | | |
|---|---|---|---|---|---|---|---|---|---|---|---|
| Sensor depth (cm) | MAGT (°C) | Sensor depth (cm) | MAGT (°C) | Sensor depth (cm) | MAGT (°C) | Sensor depth (cm) | MAGT (°C) | MAAT (°C) | TDD Sums | FDD Sums | MASD (cm) |
| 50* | --- | 10* | --- | 10 | 1.53 | 25* | --- | | | | |
| **100** | **-0.04** | 25* | --- | 50 | 0.14 | 50* | --- | 3.24 | 2009.8 | 829.1 | 2.7 |
| **200** | **-0.06** | 50* | --- | **100** | **-0.07** | 100* | --- | | | | |
| **300** | **-0.07** | 100[#]* | --- | 200[#] | -0.07 | 130* | --- | | | | |

*Thermistor or data logger failure

[#]Permafrost thaw during observation period

895 Table 2. Permafrost plateau extent mapped in each study region in 1950, 1984, 1996, and ca. 2010. Analyzed wetland area for each
896 study region is given along with the number of features, total plateau area, mean plateau area, and plateau extent for each image
897 observation year. In ca. 2010, images were acquired in 2011 (Mystery Creek and Watson Lake), 2012 (Tustumena Lake), and 2013
898 (Browns Lake).
899

| Study Region | Wetland Area (ha) | 1950 | | | | 1984 | | | | 1996 | | | | ca. 2010 | | | |
|---|---|---|---|---|---|---|---|---|---|---|---|---|---|---|---|---|---|
| | | Number of Features | Total Plateau Area (ha) | Mean Plateau Area (ha) | Plateau Extent (%) | Number of Features | Total Plateau Area (ha) | Mean Plateau Area (ha) | Plateau Extent (%) | Number of Features | Total Plateau Area (ha) | Mean Plateau Area (ha) | Plateau Extent (%) | Number of Features | Total Plateau Area (ha) | Mean Plateau Area (ha) | Plateau Extent (%) |
| Mystery Creek | 1562.0 | 212 | 511.5 | 2.4 | 32.7 | 237 | 457.7 | 1.9 | 29.3 | 335 | 292.6 | 0.9 | 18.7 | 321 | 232.3 | 0.7 | 14.9 |
| Watson Lake | 904.2 | 44 | 86.6 | 2.0 | 9.6 | 55 | 54.0 | 1.0 | 6.0 | 68 | 35.4 | 0.5 | 3.9 | 67 | 29.8 | 0.4 | 3.3 |
| Browns Lake | 1013.0 | 102 | 111.9 | 1.1 | 11.0 | 117 | 67.2 | 0.6 | 6.6 | 107 | 51.2 | 0.5 | 5.1 | 89 | 38.6 | 0.4 | 3.8 |
| Tustemena Lake | 1333.4 | 92 | 210.2 | 2.2 | 15.8 | 150 | 168.6 | 1.1 | 12.6 | 183 | 143.5 | 0.8 | 10.8 | 206 | 69.9 | 0.3 | 5.2 |
| All Sites | 4812.7 | 450 | 920.2 | 2.0 | 19.1 | 559 | 747.5 | 1.3 | 15.5 | 693 | 522.6 | 0.8 | 10.9 | 683 | 370.6 | 0.5 | 7.7 |

900

901

Table 3. Change in the extent of permafrost plateaus for each of the study regions between 1950 and ca. 2010, 1950 and 1984, 1984 and 1996, and 1996 and ca. 2010. Change is reported in aerial units per year, proportional area change, percent change per year, and by the type of change. Change type refers to whether the plateau loss occurred along the periphery of a feature (lateral), in the centre of a feature (internal), or whether complete loss of a feature occurred. In ca. 2010, images were acquired in 2011 (Mystery Creek and Watson Lake), 2012 (Tustumena Lake), and 2013 (Browns Lake).

| Study Area | Area Change (ha yr$^{-1}$) | Proportional Area Change (ha yr$^{-1}$ 100 ha$^{-1}$) | Percent Change (% yr$^{-1}$) | Change Type | | |
|---|---|---|---|---|---|---|
| **1950 to ca. 2010** | | | | Lateral (%) | Internal (%) | Complete (%) |
| Mystery Creek | -4.6 | -0.3 | -0.9 | 86.2 | 3.3 | 10.5 |
| Watson Lake | -0.9 | -0.1 | -1.1 | 90.9 | 0.8 | 8.3 |
| Browns Lake | -1.2 | -0.1 | -1.0 | 77.2 | 0.3 | 22.4 |
| Tustumena Lake | -2.3 | -0.2 | -1.1 | 86.0 | 1.7 | 12.3 |
| All Sites | -9.2 | -0.2 | -1.0 | 85.1 | 1.5 | 13.4 |

| Study Area | Area Change (ha yr$^{-1}$) | Proportional Area Change (ha yr$^{-1}$ 100 ha$^{-1}$) | Percent Change (% yr$^{-1}$) | Change Type | | |
|---|---|---|---|---|---|---|
| **1950 to 1984** | | | | Lateral (%) | Internal (%) | Complete (%) |
| Mystery Creek | -1.6 | -0.1 | -0.3 | 88.8 | 5.2 | 5.9 |
| Watson Lake | -1.0 | -0.1 | -1.1 | 91.7 | 1.4 | 6.9 |
| Browns Lake | -1.3 | -0.1 | -1.2 | 89.0 | 0.6 | 10.1 |
| Tustumena Lake | -1.2 | -0.1 | -0.6 | 94.1 | 2.1 | 3.8 |
| All Sites | -5.1 | -0.1 | -0.6 | 91.0 | 2.3 | 6.7 |

| Study Area | Area Change (ha yr$^{-1}$) | Proportional Area Change (ha yr$^{-1}$ 100 ha$^{-1}$) | Percent Change (% yr$^{-1}$) | Change Type | | |
|---|---|---|---|---|---|---|
| **1984 to 1996** | | | | Lateral (%) | Internal (%) | Complete (%) |
| Mystery Creek | -13.8 | -0.9 | -3.0 | 87.1 | 1.8 | 11.2 |
| Watson Lake | -1.6 | -0.2 | -2.9 | 88.7 | 0.6 | 10.7 |
| Browns Lake | -1.3 | -0.1 | -2.0 | 84.0 | 0.1 | 16.0 |
| Tustumena Lake | -2.1 | -0.2 | -1.2 | 85.1 | 2.9 | 12.0 |
| All Sites | -18.7 | -0.4 | -2.5 | 86.2 | 1.3 | 12.5 |

| Study Area | Area Change (ha yr$^{-1}$) | Proportional Area Change (ha yr$^{-1}$ 100 ha$^{-1}$) | Percent Change (% yr$^{-1}$) | Change Type | | |
|---|---|---|---|---|---|---|
| **1996 to ca. 2010** | | | | Lateral (%) | Internal (%) | Complete (%) |
| Mystery Creek | -4.0 | -0.3 | -1.4 | 82.7 | 3.0 | 14.3 |
| Watson Lake | -0.4 | -0.1 | -1.1 | 92.2 | 0.5 | 7.3 |
| Browns Lake | -0.7 | -0.1 | -1.4 | 58.7 | 0.1 | 41.2 |
| Tustumena Lake | -4.6 | -0.3 | -3.2 | 78.7 | 0.2 | 21.1 |
| All Sites | -9.5 | -0.2 | -1.8 | 78.1 | 1.0 | 21.0 |

911 Table 4. Mean annual, mean summer (May to September), and mean winter (October to April) air
912 temperature for the three remotely sensed image observation periods compiled from the Kenai
913 Municipal Airport (WBAN 26523) and estimated from the MRC station (Kenai 29 ENE - AWS
914 702590).
915

| Remote Sensing Time Period | Mean Annual Air Temperature (°C) | | Mean Summer Air Temperature (°C) | | Mean Winter Air Temperature (°C) | |
|---|---|---|---|---|---|---|
| | Kenai Airport | MRC | Kenai Airport | MRC | Kenai Airport | MRC |
| 1950 to 1984 | 1.12 | 0.59 | 9.92 | 10.39 | -5.29 | -6.54 |
| 1984 to 1996 | 1.77 | 1.31 | 10.28 | 10.78 | -4.37 | -5.52 |
| 1996 to 2015 | 2.34 | 1.86 | 10.81 | 11.31 | -3.77 | -4.95 |

916

917 **Figures**
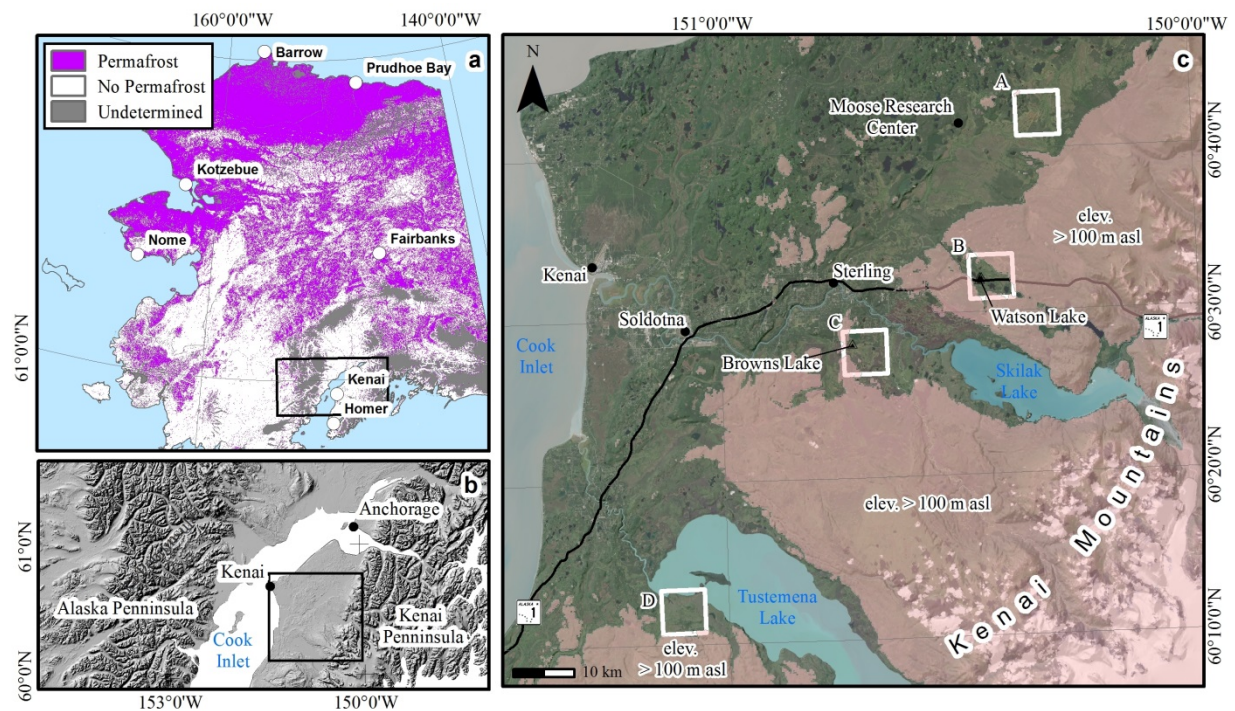
918

919 Figure 1: Study area figure. (a) Recent permafrost map of Alaska (Pastick et al., 2015) indicating
920 permafrost presence (purple) and absence (white) in the upper one meter of the ground surface.
921 (b) Hillshade relief image showing a portion of southcentral Alaska. The study region on the Kenai
922 Peninsula lowlands is shown with the black box outline. (c) The portion of the Kenai Peninsula
923 lowlands where field studies and remotely sensed observations were conducted. Ground
924 temperature observations were collected at the Browns Lake and Watson Lake sites. The remote
925 sensing change detection areas are shown with a white box: (A) Mystery Creek, (B) Watson Lake,
926 (C) Browns Lake, and (D) Tustumena Lake wetland complexes.

927
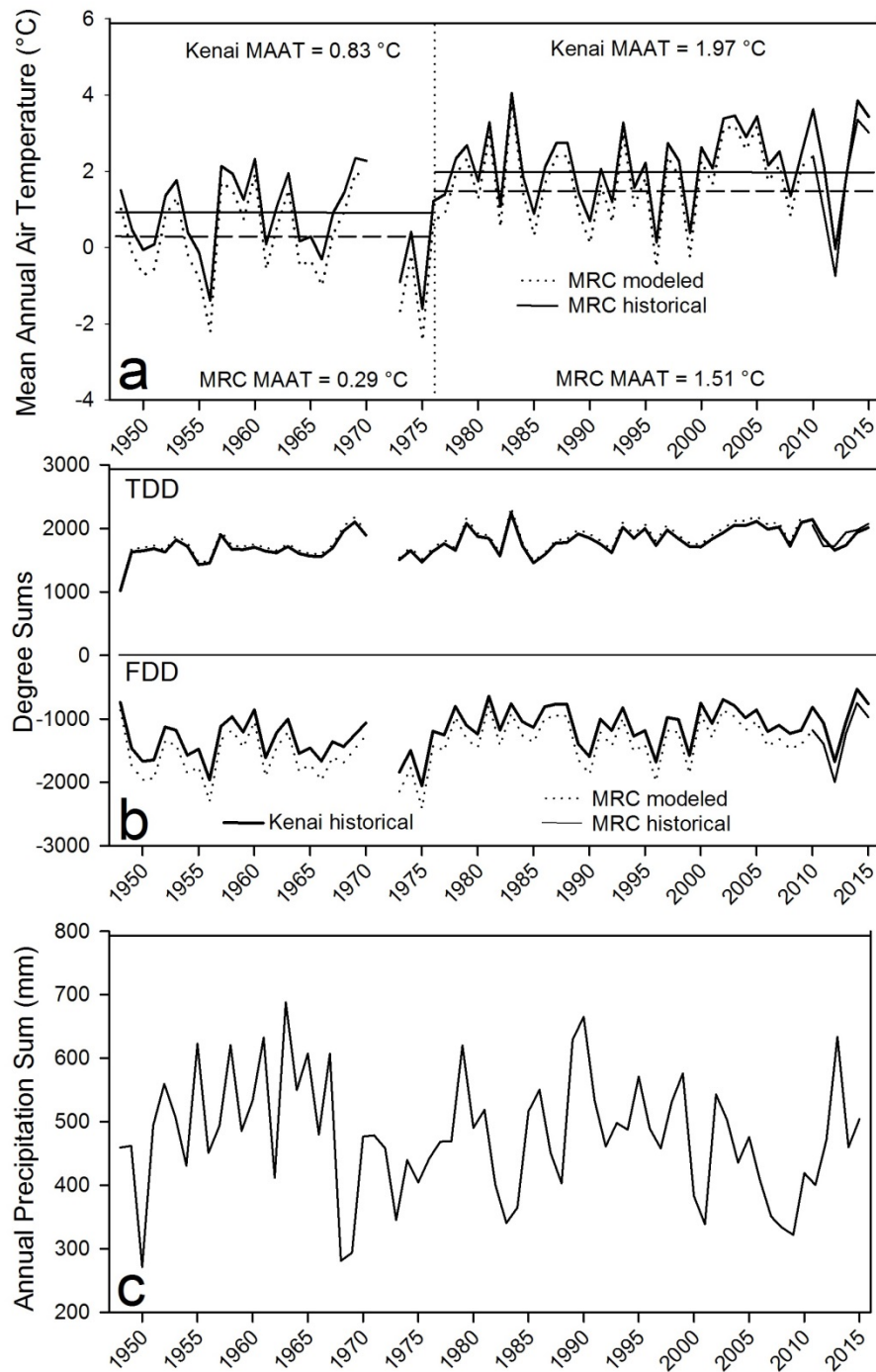
Figure 2: a) Historical (1948-2015) mean annual air temperature compiled from Kenai Municipal Airport (WBAN 26523) hourly surface data and interpolated (broken) and measured (solid) mean annual air temperature for the MRC station (Kenai 29 ENE AWS 702590).  b) Thawing degree day (TDD) and freezing degree day (FDD) sums for 1948-2015 derived from historical and interpolated daily mean temperature.  c) Cumulative annual precipitation data from the Kenai Municipal Airport (WBAN 26523) between 1948 and 2015.

934

935

Figure 3:  Field photos of residual permafrost plateau landforms and thermokarst on the western Kenai Peninsula lowlands.  (a) A forested permafrost plateau in the Browns Lake wetland complex.  A thermokarst moat and drowning black spruce trees in the (b) Browns Lake and (c) Watson Lake wetland complexes.

940

941

942
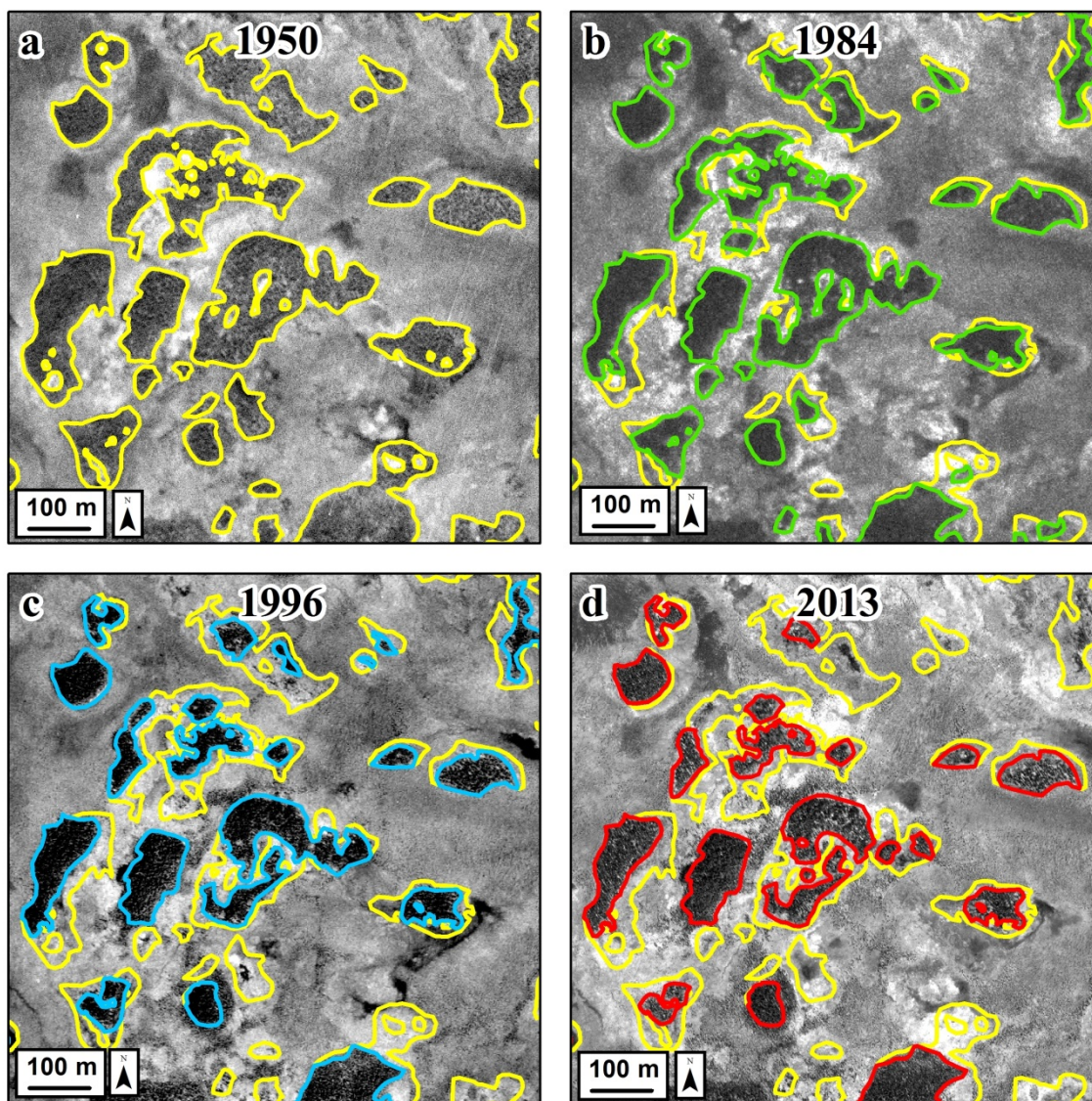
Figure 4: Time series documenting the extent of a subset of permafrost features in the Browns Lake wetland complex in (a) 1950, (b) 1984, (c) 1996, and (d) 2013. Permafrost plateau extent in 1950 is shown as a yellow polygon in each frame and other time slices outlined as green (1984), blue (1996), and red (2013).

947
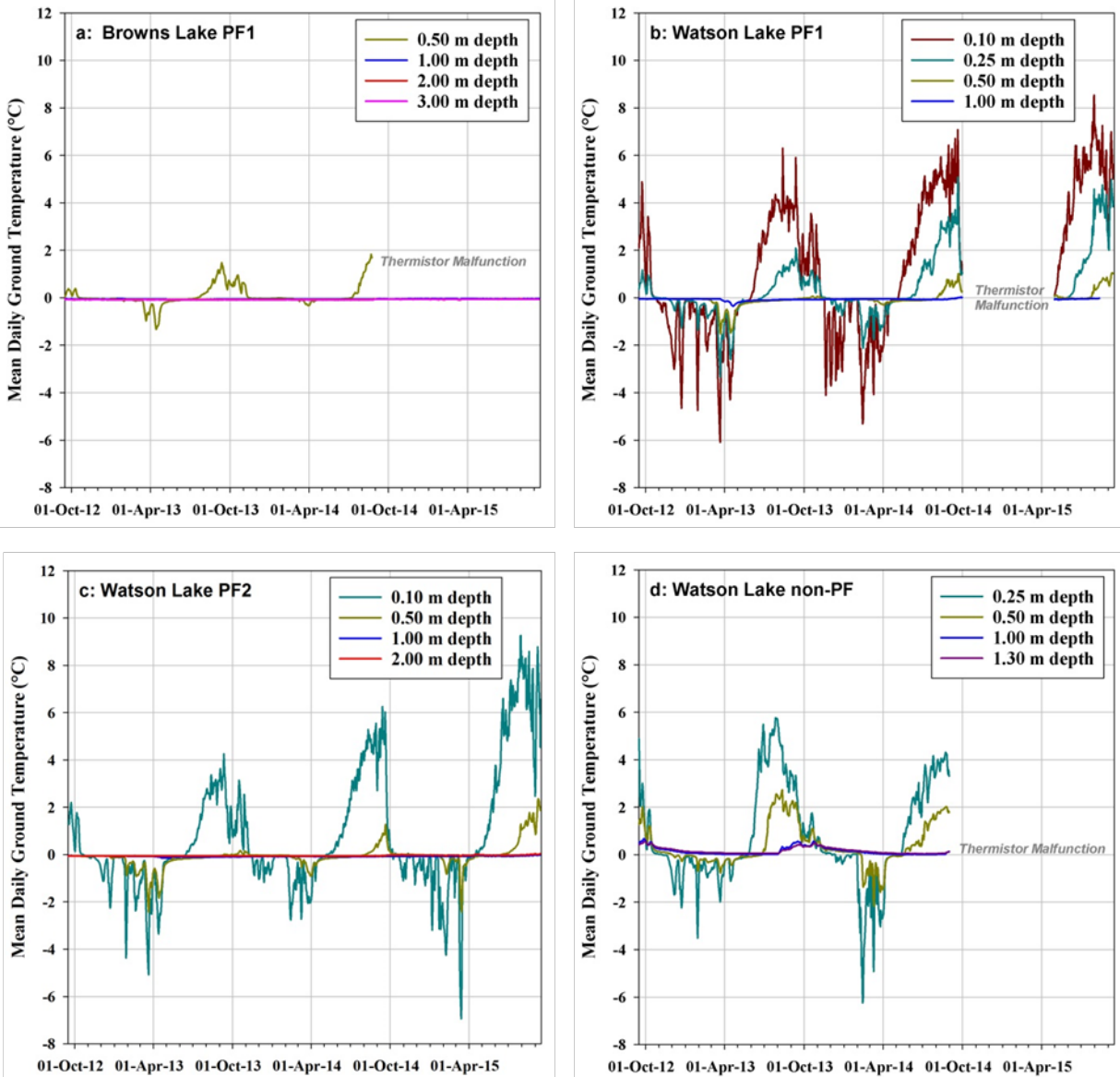
Figure 5: Mean daily ground temperature data plots for the four shallow boreholes on the western
Kenai Peninsula lowlands for the period of 16 September 2012 to 15 September 2015: (a) Browns
Lake PF1 site, (b) Watson Lake PF1 site, (c) Watson Lake PF2 site, and (d) Watson Lake non-PF
site. All axes scales are the same but sensor depths vary among sites based on site characteristics.
Missing data indicates sensor or thermistor failure.

954

955
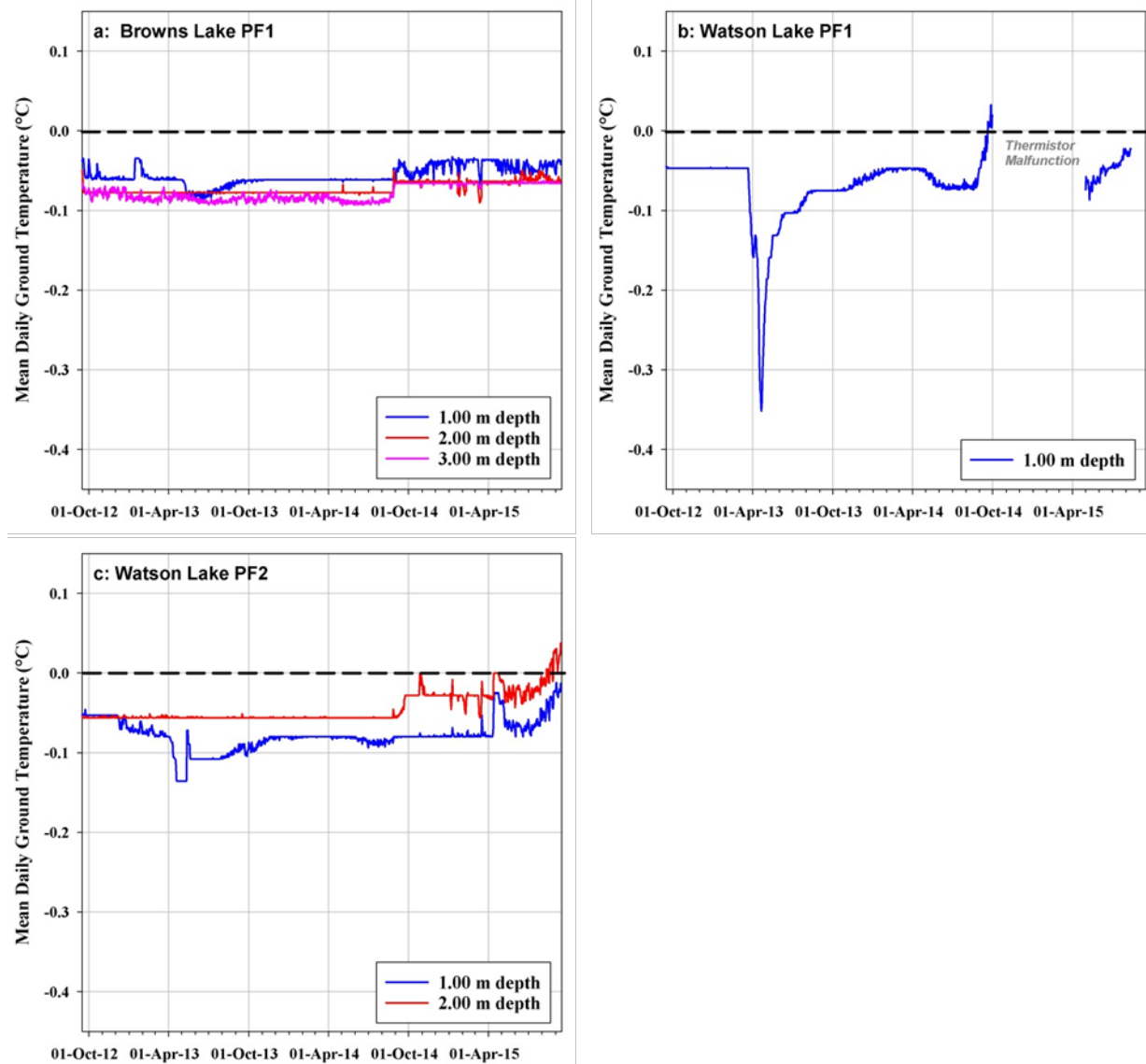
Figure 6:  Mean daily ground temperature data plots indicating the presence of permafrost on the western Kenai Peninsula lowlands for the period of 16 September 2012 to 15 September 2015:  (a) Browns Lake PF1 site, (b) Watson Lake PF1 site, and (c) Watson Lake PF2 site.  Top-down permafrost thaw occurred at Watson Lake PF1 during the fall of 2014 and bottom-up permafrost thaw occurred at Watson Lake PF2 during the fall of 2015.

961

962
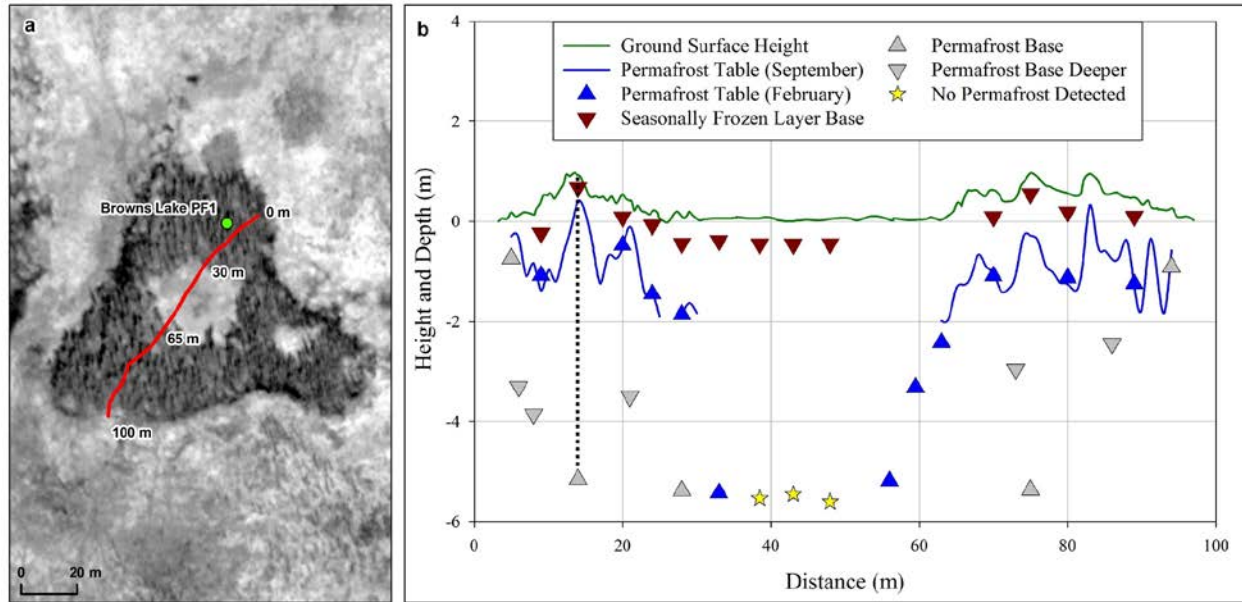
Figure 7: (a) High-resolution satellite image showing the permafrost plateau in the Browns Lake wetland complex where detailed field surveys were conducted as well as the location of the Browns Lake PF1 data logger (green dot). (b) A ~100 m transect across the Browns Lake PF1 permafrost plateau site showing ground surface height above the wetland (green line), depth to the permafrost table (blue line and blue arrows), permafrost thickness constraints (grey arrows), seasonally frozen ground depth (maroon arrows), and lack of permafrost (yellow stars) as measured by probing, drilling, and coring. Locations where the permafrost table exceeded 2.2 m from the ground surface (limiting depth for September surveys) are indicated with a non-existent blue line. Locations where the base of the permafrost was encountered are indicated with an upward looking grey triangle and those locations where it was not encountered, a downward looking grey triangle. The black dashed vertical line represents the location of the PF-BL-6 permafrost core.
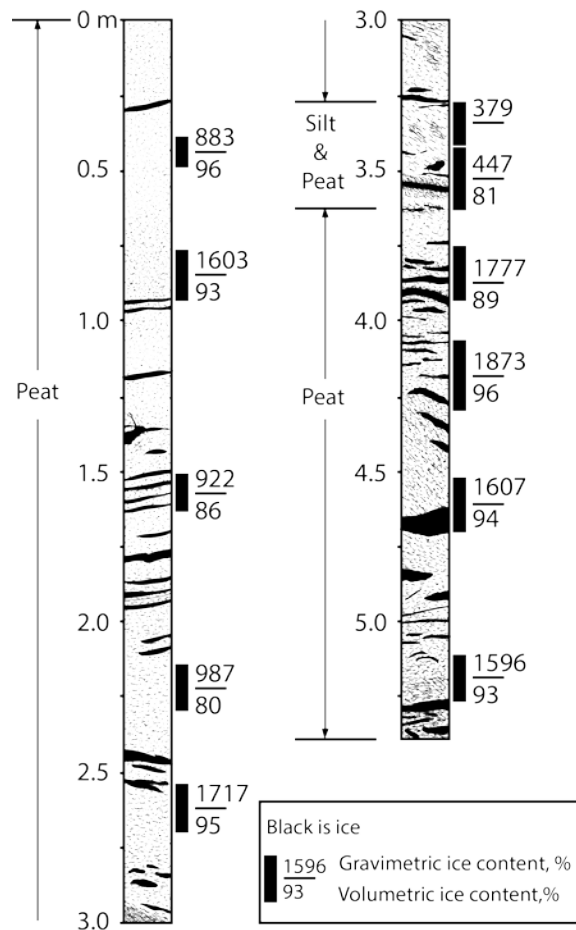
974
975
976 Figure 8: Cryostratigraphy and ice contents from borehole PF-BL-6 (inspired by Kanevskiy et
977 al., 2014). The gravimetric and volumetric ice contents of the peat varied between 883–1873%
978 and 80–96%, respectively, while they were 379–447% and 81%, respectively, in the silt and peat
979 layer located between 3.32 m and 3.65 m.

Figure 9: (a) Stratigraphic contact between the base of the frozen silt and peat layer occurring at 3.65 m and the underlying frozen peat. (b) Example of organic-matrix microlenticular to suspended cryostructures developed in the peat below the stratigraphic contact shown in (a).
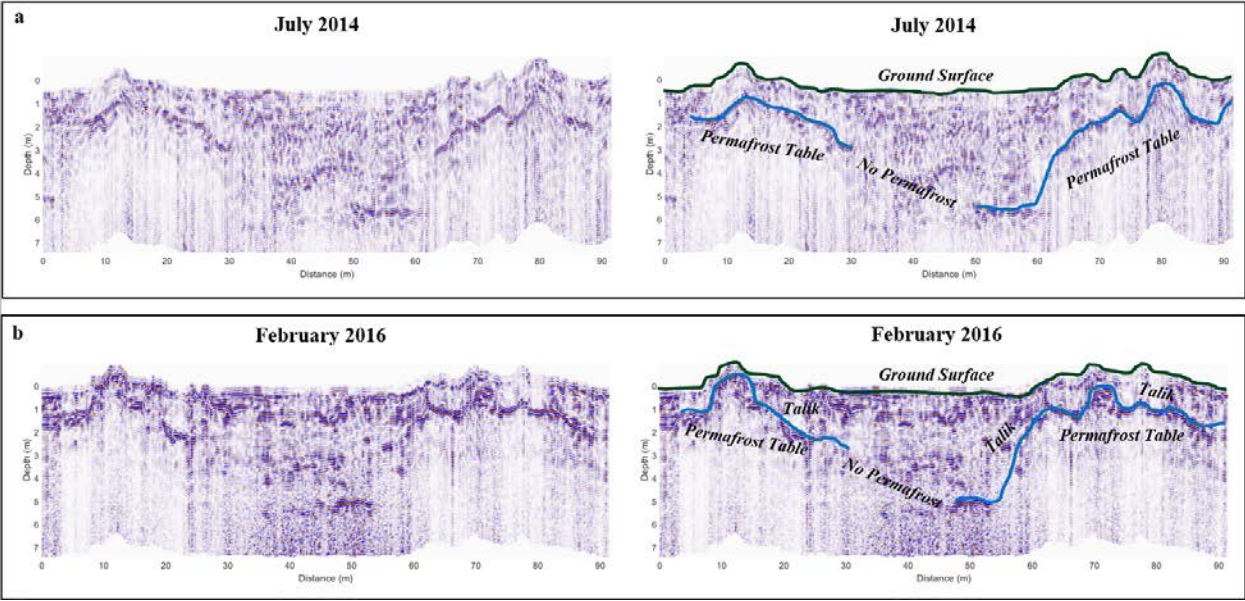
Figure 10: GPR profiles at the intensive Browns Lake permafrost plateau (Fig. 7a) from a) late-July 2014 with Mala shielded 100-MHz antennas and b) mid-February 2016 with Sensors & Software unshielded bi-static 100-MHz antennas. Processed radargrams are on the left and processed, interpreted radargrams are on the right. Both summer and winter profiles clearly show reflectors associated with the permafrost table and in the case of (b) show the presence of a talik. However, we were unable to image the permafrost base using GPR. Note that the two GPR transects differ slightly in their orientation across the feature.

**Loss between 1950 and 1984**  **Loss between 1996 and ca. 2010**

**Loss between 1984 and 1996**  **Permafrost plateau extent ca. 2010**

995
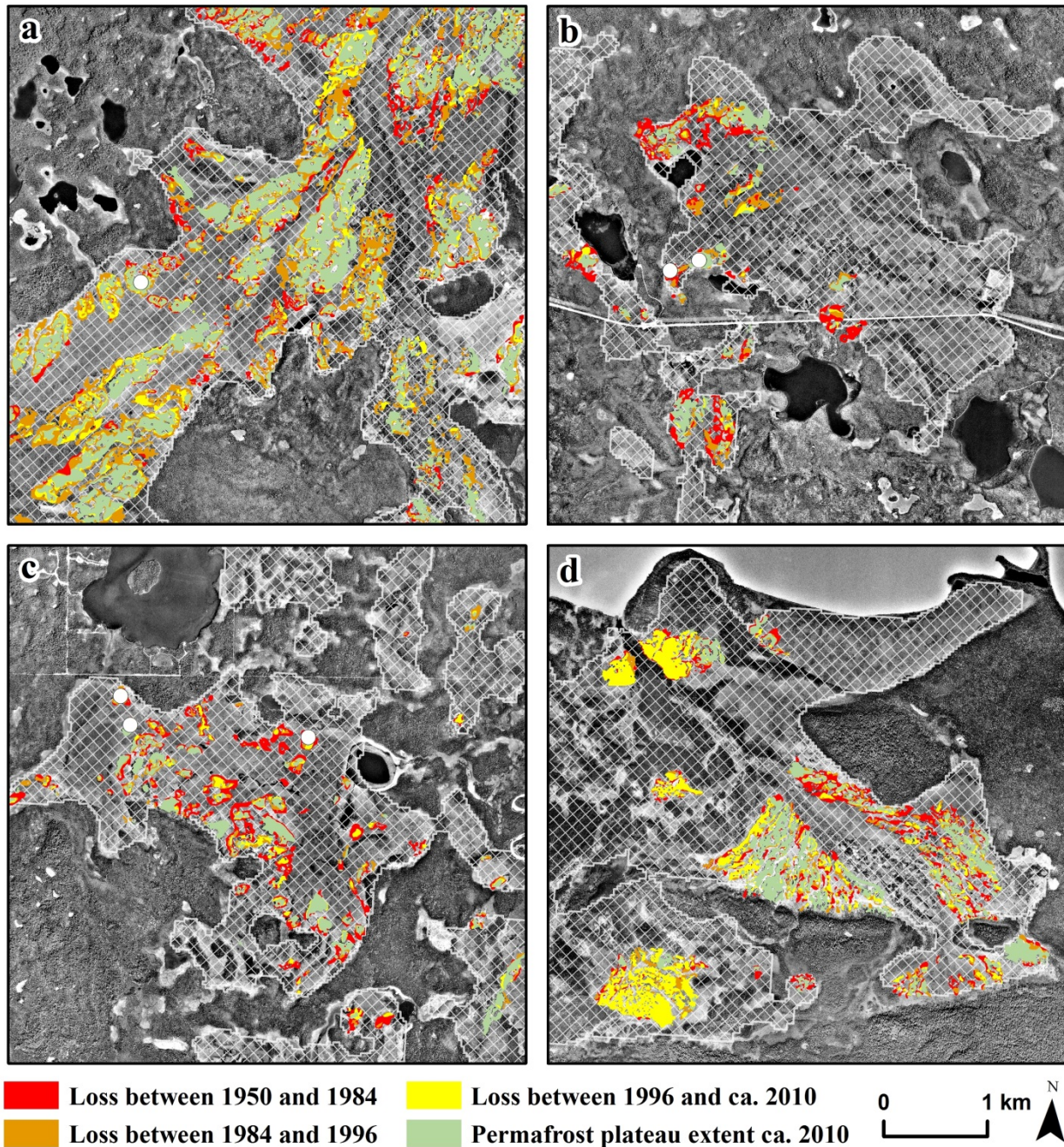
Figure 11: Spatial and temporal pattern of permafrost loss within four change detection areas: a) Mystery Creek, b) Watson Lake, c) Browns Lake, and d) Tustumena Lake. Red indicates feature loss between 1950 and 1980, orange is feature loss between 1984 and 1996, yellow is feature loss between 1996 and ca. 2010, and green is ca. 2010 permafrost plateau extent. The white dots indicate the location of field verified permafrost between 2009 and 2016. The hatched white polygons indicate the wetland extent where plateau features were mapped in each study area. Background imagery is the 1996 orthophotography.